



저작자표시-비영리-변경금지 2.0 대한민국

이용자는 아래의 조건을 따르는 경우에 한하여 자유롭게

- 이 저작물을 복제, 배포, 전송, 전시, 공연 및 방송할 수 있습니다.

다음과 같은 조건을 따라야 합니다:



저작자표시. 귀하는 원저작자를 표시하여야 합니다.



비영리. 귀하는 이 저작물을 영리 목적으로 이용할 수 없습니다.



변경금지. 귀하는 이 저작물을 개작, 변형 또는 가공할 수 없습니다.

- 귀하는, 이 저작물의 재이용이나 배포의 경우, 이 저작물에 적용된 이용허락조건을 명확하게 나타내어야 합니다.
- 저작권자로부터 별도의 허가를 받으면 이러한 조건들은 적용되지 않습니다.

저작권법에 따른 이용자의 권리는 위의 내용에 의하여 영향을 받지 않습니다.

이것은 [이용허락규약\(Legal Code\)](#)을 이해하기 쉽게 요약한 것입니다.

[Disclaimer](#)

공학석사 학위논문

Person Identification and
Authentication with Short-time
measured
Electroencephalography

단시간 측정 뇌파를 이용한 개별 인식 및 개인
인증

2015년 2월

서울대학교 대학원
협동과정 바이오엔지니어링 전공
한 정 민

Person Identification and
Authentication with Short-time
measured
Electroencephalography

지도교수 박 광 석

이 논문을 공학석사 학위논문으로 제출함

2014년 12월

서울대학교 대학원

협동과정 바이오엔지니어링 전공

한 정 민

한정민의 공학석사 학위논문을 인준함

2015년 1월

위 원 장 _____ (인)

부위원장 _____ (인)

위 원 _____ (인)

ABSTRACT

Person Identification and Authentication with Short-time measured Electroencephalography

Chungmin Han

The Interdisciplinary Program of Bioengineering
The Graduate School
Seoul National University

This thesis proposes a method of distinct person identification and authentication using short-time measured electroencephalography (EEG) designed to have a low error rate. The evaluations are focused on practicality of the measurement process and stability of the connectivity features over time of repeatedly measured EEG at different times along with performances.

First, the uniqueness of the features extracted, specifically, power spectrum density (PSD) and z -transformed coherence (ZCOH), are estimated by applying leave-one-out cross

validation on data used as the training set. A frequency range of 1–40 Hz is selected from the training results to achieve the best classification accuracy in the testing process. The K–nearest neighbor method is used as the classifier with correlation modified Euclidean distance measurements. Using PSD only, the best correct recognition rate achieved in the 1–40 Hz range is 98.83%, whereas for ZCOH, the best correct recognition rate achieved in the range is 99.67%. Consequently, we conclude that PSD and ZCOH contain uniqueness of individuals.

Second, an authentication testing process is conducted with EEG measured over two days and its performance is evaluated. Two types of design modes commonly used in biometrics are applied in this thesis: “Registered only” mode and “Imposter” mode. The former mode focuses on whether the test data are well classified to their correct class; therefore, correct recognition rate (CRR) is calculated for overall performance along with the precision, recall, specificity, and F–score for each subject. Consequently, for PSD and ZCOH, averages of 81.35% and 80.04% for precision, 78.20% and 74.88% for recall, 99.04%

and 98.81% for specificity, and 0.78 and 0.75 for F-score are achieved at correct recognition rates of 80.39% and 75.70%. The latter, “Imposter,” mode is designed with a threshold in order to consider the case of other people trying to authenticate. The threshold is selected empirically. To evaluate this mode, false acceptance rate (FAR), false rejection rate (FRR), and half of total error rate (HTER), are calculated. The lowest HTERs achieved for PSD and ZCOH are 13.55% and 19.98%, respectively.

Finally, statistical analysis of ZCOH is conducted by inspecting the results of authentication tests in order to filter coherence values that guarantee stability and significance. Filtering combinations of coherence for each subject’s frequency bands is achieved by conducting analysis of variance (ANOVA) on data measured on three different days.

The results confirm that reliable person identification and authentication with short-time measured EEG using the proposed simple method can be practically adopted and utilized in various applications.

Keywords: electroencephalography, biometrics, personal
recognition

Student number: 2013-21042

CONTENTS

| | |
|---|-----------|
| Abstract | i |
| Contents..... | v |
| List of Tables..... | viii |
| List of Figures | ix |
| Chapter 1 Introduction..... | 1 |
| 1.1 Biometrics and applications | 2 |
| 1.2 Attributes of biometrics | 6 |
| 1.3 Electroencephalography (EEG) | 9 |
| 1.4 EEG as a biometric: Related studies | 11 |
| 1.5 Purpose of this study | 14 |
| Chapter 2 Methods | 16 |
| 2.1 Electroencephalography measurement | 16 |
| 2.2 Experimental protocol..... | 19 |
| 2.3 Design of the authentication system | 20 |
| 2.3.1 Artifact rejection and signal pre-processing..... | 22 |
| 2.3.2 Feature extraction..... | 24 |
| 2.3.2.1 Power spectrum density | 24 |

| | |
|--|-----------|
| 2.3.2.2 Z-transformed coherence | 25 |
| 2.3.2.3 Feature evaluation of uniqueness | 28 |
| 2.3.2.4 Frequency range selection | 29 |
| 2.3.3 Training and testing | 30 |
| 2.3.4 Classification..... | 31 |
| 2.3.5 Performance Evaluation..... | 35 |
| 2.3.5.1 Registered only mode | 35 |
| 2.3.5.2 Imposter mode | 35 |
| 2.4 Stability evaluation statistics | 38 |
| Chapter 3 Results | 40 |
| 3.1 Details of materials used..... | 40 |
| 3.2 Feature vectors and evaluation | 44 |
| 3.2.1 Power spectrum density | 44 |
| 3.2.2 Z-transformed coherence | 47 |
| 3.2.3 Uniqueness evaluation (LOOCV)..... | 50 |
| 3.2.3.1 Result of power spectrum density | 50 |
| 3.2.3.2 Result of Z-transformed coherence..... | 53 |
| 3.2.3.3 Frequency range selection | 53 |
| 3.3 Authentication test evaluation | 56 |
| 3.3.1 Registered only mode | 56 |
| 3.3.1.1 Power spectrum density..... | 57 |
| 3.3.1.2 Z-transformed coherence..... | 57 |
| 3.3.2 Imposter mode..... | 60 |
| 3.3.2.1 Power spectrum density..... | 61 |

| | |
|--|-----------|
| 3.3.2.2 Z-transformed coherence..... | 65 |
| 3.4 Stability evaluation statistics | 69 |
| 3.4.1 Significant Z-coherence of individuals..... | 70 |
| Chapter 4 Discussion | 74 |
| 4.1 Factors that influence EEG | 76 |
| 4.2 Coherence characteristics in resting state | 76 |
| 4.3 Major drawback of using EEG as a biometric | 77 |
| 4.4 Limitations of the present study..... | 78 |
| Chapter 5 Conclusion | 80 |
| References..... | 81 |
| Abstract in Korean | 87 |

LIST OF TABLES

| | |
|---|----|
| Table 1 Attributes for biometric | 8 |
| Table 2 Performance evaluation of the authentication system | 37 |
| Table 3 General information pertaining to the subjects who participated and the interval (days) of measurements..... | 41 |
| Table 4 Number of trials used in the tests for each subject.... | 43 |
| Table 5 PSD LOOCV CRR with different frequency ranges and varying k-values | 51 |
| Table 6 ZCOH LOOCV CRR with different frequency ranges and varying k values..... | 54 |
| Table 7 Identification performance of test data for each subjects using PSD (1–40 Hz) | 58 |
| Table 8 Identification performance of test data for each subjects using ZCOH (1–40 Hz) | 59 |
| Table 9 Imposter mode: FRR and FAR of test data using PSD (1–40 Hz) with varying thresholds..... | 62 |
| Table 10 Imposter mode: FRR and FAR of test data using ZCOH (1–40 Hz) with varying thresholds..... | 66 |

LIST OF FIGURES

| | |
|--|----|
| Figure 1 Examples of biometrics and its applications: (a) Palm print (b) Fingerprints at immigration customs (c) PayPal with face recognition (d) iPhone with fingerprint recognition (e) Motion (f) Nymi wearable ECG identification | 5 |
| Figure 2 (a) General adult EEG rhythms, (b) their characteristics | 10 |
| Figure 3 EEG measurement setup (a) (left) g.USBamp, (right) EEG cap on subject, (b) montage of 32 channels (10–20 system) | 18 |
| Figure 4 Measurement repetition interval | 19 |
| Figure 5 Flow of operations in the authentication system | 21 |
| Figure 6 Feature extraction from EEG signal: (a) Power spectrum density feature of each channel, (b) Z-transformed coherence of two channels | 27 |
| Figure 7 Classification method used in the “Registered only” mode: (a) Power spectrum density based, (b) Z-transformed coherence based | 32 |
| Figure 8 Decision process in “Imposter” mode: (a) Power spectrum density based, (b) Z-transformed coherence based | 34 |

| | |
|--|----|
| Figure 9 Description of false acceptance rate and false reject rate with level of sensitivity | 37 |
| Figure 10 Process description of statistical test..... | 39 |
| Figure 11 Example PSD of rejected trial and regular trial | 43 |
| Figure 12 PSD feature plots of training data: S09 (a) 1–15 channels (Occipital & Parietal), (b) 16–30 channels (Central & Frontal) | 45 |
| Figure 13 PSD plot of a single channel (O1) for each of the 20 subjects | 46 |
| Figure 14 Z-coherence plot of the training data for a single subject. Combinations of ch1 to ch10..... | 47 |
| Figure 15 ZCOH plot of a single combination (Fp1 & Fp2) for each of the 20 subjects..... | 49 |
| Figure 16 PSD: Correct recognition rate with fixed frequency range and varying k-values..... | 51 |
| Figure 17 PSD: Correct recognition rate for all frequency ranges and k-values. (a) k = 1, (b) k = 5, (c) k = 7, (d) k = 10 and (e) k = 20 | 52 |
| Figure 18 ZCOH: Correct recognition rate (%) with fixed frequency range and varying value..... | 54 |
| Figure 19 ZCOH: Correct recognition rate for all frequency ranges and k-values. (a) k = 1, (b) k = 5, (c) k = 7, (d) k = 10, | |

| | |
|---|----|
| and (e) $k=20$ | 55 |
| Figure 20 PSD Imposter: (a) False rejection rate, (b) false acceptance rate plot (Labeled is at threshold 0.7) | 63 |
| Figure 21 PSD Imposter: Half total error rate (Labeled is at threshold 0.7)..... | 64 |
| Figure 22 ZCOH Imposter: (a) false rejection rate, (b) false acceptance rate plot (Label is at threshold 0.9) | 67 |
| Figure 23 ZCOH Imposter: Half of total error rate (Labeled is at threshold 0.9)..... | 68 |
| Figure 24 Theta coherence map of the subjects..... | 71 |
| Figure 25 Alpha coherence map of the subjects..... | 72 |
| Figure 26 Beta coherence map of the subjects..... | 73 |

CHAPTER 1. INTRODUCTION

Biometrics refers to the identifying of individuals using unique physical attributes detected and recorded by an electronic device or system. As the world becomes smaller as a result of the Internet transcending the limitations of physical distance, security of personal information is becoming increasingly important. In the past, securing confidential information by limiting physical access was enough to reduce the risk of information being stolen. However, following the development of computers and generalization of the Internet, electronic encryption became an advanced method of securing information and identifying individuals. However, electronic encryption is susceptible to being hacked or copied. Thus, to overcome this disadvantage, many studies have been conducted on various types of biometrics that are unique to individuals, and at the same time have a low risk of being stolen, for use as a means of personal identification and authentication.

1.1 Biometrics and applications

Recently, many systems in various fields have had biometrics applied as a means of identification and authentication of individuals, resulting in reduced costs and decreased risks. Typically, the fingerprints and palm prints of newborn babies are recorded in the birth registration process and thumbprint is being placed on the backside of the identification card. Fingerprint recognition systems are also being utilized in automatic immigration customs at airports for user who agree to provide the information for a database of fingerprints. In the financial area, authentication of persons can be applied in automated teller machines and can be utilized even when the user is without their other verification materials. Recently, PayPal, a global electronic payment system, has been trying to adopt a face recognition system to verify payment as a means of reducing its cumbersome authentication process [1]. Other areas such as election administration, establishment of databases to aid in the identification of serious criminals, and personal medical records

can adopt biometrics for more efficient and cost-reduced management.

Further, applications that regard legal validity, smartphones, and wearable devices are also adopting biometrics to provide security. The most widely publicized example in recent times is the installation of a fingerprint recognition sensor on the iPhone5S in 2013, restricting authorized access only to registered users [2]. Nymi, a wearable device, also identifies and authenticates recorded electrocardiograph (ECG) to provide personal security [3].

The idea of using biometrics for identification and authentication is attractive because the user does not need to carry any additional token or memorize electronic passwords. However, biometrics such as fingerprints, iris, signature motion, and voice recognition all are at risk of being duplicated, which can lead to false authentication. Thus, bio-signals are being examined as candidates for biometrics because they are virtually impossible to copy. However, due to the intra-variance of bio-signals,

extracting features to identify distinct individuals and assuring stable authentication remains a challenge.



(a)



(b)



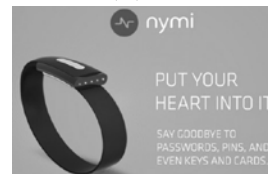
(c)



(d)



(e)



(f)

Figure 1. Examples of biometrics and its applications: (a) Palm print [4] (b) Fingerprints at immigration customs [5] (c) PayPal with face recognition [1] (d) iPhone with fingerprint recognition [2] (e) Motion [6] (f) Nymi wearable ECG identification [3]

1.2 Attributes of biometrics

There are several requirements for bio-signals to be eligible for utilization in biometrics. These are universality, uniqueness, permanence, performance, collectability, acceptability, and circumvention. Universality is the possibility of bio-signals being measured from everyone. Uniqueness is the main property and assumption used to compose personal recognition. Permanence signifies the stability of biometrics to be applied over an extended period of time. As regards permanence, bio-signals are at a disadvantage because they can vary according to physiological/psychological factors. Performance is the base factor for biometrics when applied in practical situations. Collectability measures the ease with which bio-signals are acquired in the authentication process. Lastly, circumvention represents the risk level of an item being stolen or duplicated.

Bio-signals, especially ECG and EEG satisfy universality and have a major advantage in the aspect of circumvention. Thus, many studies have been conducted to extract features from these

signals in order to distinguish individuals and to examine stability from the aspect of permanence [7-9].

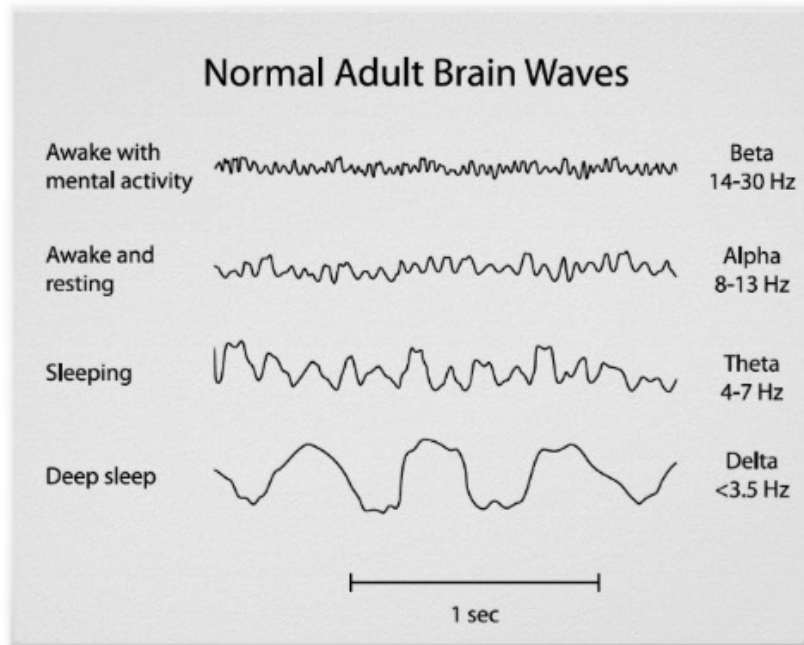
Table 1. Attributes for biometric

| Attributes | Description |
|---------------------------|--|
| (1) Universality | Each person should have that characteristic |
| (2) Uniqueness | Any two person should be different in terms of the characteristic |
| (3) Permanence | Characteristics should be sufficiently invariant over a period of time |
| (4) Performance | Ensuring good performance |
| (5) Collectability | Characteristic should be quantitatively measurable with some practical device |
| (6) Acceptability | The public should have no strong objection to the measuring/collecting of the characteristic |
| (7) Circumvention | Characteristic should be robust to attacks |

1.3 Electroencephalography (EEG)

EEG is non-invasive recording of the electrical activity of the brain, and was first introduced in 1924 by Hans Berger [10]. EEG measures voltage fluctuations resulting from ionic current flows within the neurons of the brain and represents its physiological conditions. EEG has been applied in various clinical forms of analyses to diagnose mental disease/brain lesions and to confirm brain death [11–13].

The EEG of a healthy adult is composed of several frequency ranges representing different functions (see Figure 2). Delta waves are seen during slow-wave sleep and theta waves are seen when adults are drowsy. Alpha rhythms are known to be dominant when the eyes are closed and are associated with inhibition control. Beta rhythms represent active thinking and gamma rhythms are associated with short-term memory and multimodal sensory processing.



(a)

| Activity | Frequency | Brain State |
|-----------------|------------------|-----------------------|
| <i>delta</i> | 0.5-4 Hz | sleeping/unconscious |
| <i>theta</i> | 4-8 Hz | imagination |
| <i>alpha</i> | 8-12 Hz | calm consciousness |
| <i>beta</i> | 12-35 Hz | focused consciousness |
| <i>gamma</i> | >35 Hz | peak performance. |

(b)

Figure 2. (a) General adult EEG rhythms, (b) their characteristics.

1.4 EEG as a biometric: Related studies

Recent up-to-date studies that consider EEG as a biometric can be classified into two groups: those that determine whether EEG contains unique characteristics distinguish individuals, and those that determine whether the features of EEG remain stable over long the term with the assumption that no mental illness has occurred.

The uniqueness of individuals can be attributed to genetics. The study of twins has proven to be a great help in interpreting EEG as phenotype. Davis and Davis determined that the EEGs of resting monozygotic twins were identical by investigating such twins and comparing the results to those for dizygotic twins, which were found to be significantly more similar than those of unrelated subjects [14, 15].

These results subsequently led to studies that utilized resting EEG to recognize different individuals. It has been found that eyes-closed state EEG reflects more individual traits than eyes-open state EEG [8]. In addition to using resting EEG, event-related potentials have been applied as a means of

recognition [16]. However, because of the requirements for repeated presentation of external stimuli to induce event-related potentials, the resting EEG protocol is more widely applied.

Several researchers have proposed approaches to overcome the major drawback of collecting EEG, which requires conductive gel, by reducing the number of electrodes. Van et al. recognized 23 individuals using Fp1 and Fp2 measurement sites with 20% equal error rate (EER), and Bin et al. differentiated 11 individuals from 11 imposters using the Cz and A2 channels with a maximum of 94.60% true authentication rate [17, 18].

The studies cited above mainly used features extracted from power spectrum density such as peak frequency value and ratio of frequency range. In more recent research activities, La Rocca et al. revealed that coherence information can recognize 108 distinct subjects with a 100 % correct recognition rate by applying the feature fusion method [19].

Another main research theme is examination of the test-retest reliability of extracted power spectrum features. A study conducted by Kondacs et al. examined the variance of features

such as absolute and relative power, median and peak frequency, and the entropy extracted from the EEG of 45 healthy subjects over intervals of 25–62 months [20]. They concluded that intra–individual variation was less significant than inter–individual variations. Nöpflin et al. also considered test–retest reliability and conducted eyes–closed investigations on 20 people during two EEG recording sessions over a mean duration of 15 months [21]. They concluded that the alpha sub–band peak dominated over time. Another research focused on variations in EEG associated with circadian rhythm and caffeine intake and concluded that intra–variation of resting EEG is affected by diverse physiological conditions [22].

These results from previous studies show that resting EEG can be applied for distinct personal recognition and, at the same time, guarantee stable authentication for authentication systems designed considering intra–variance over time.

1.5 Purpose of this study

This thesis designs and evaluates an authentication system utilizing short-time measured EEG. This is contrast to previous studies, which requires either repeated measure to evoke responses or 60-seconds measurement that is not practical in real situations. In our study, EEGs are measured in eyes-closed condition for 10 seconds. The features extracted enable identification of distinct individuals and its performance is evaluated as giving stable authentication. Another drawback of previous studies is that to date, personal identification performances are evaluated by performing cross-fold validation and in the rate of test-retest reliability, which lacks evaluation of reproducibility. For this reason and practicality of personal recognition, proposed system is designed to be trained with EEG measured on the first day and tested with data measured on different days.

This remainder of this thesis is organized as follows:

Chapter 2 describes the methodology employed to measure resting EEG on different days and to compose the overall recognition system. Experimental setups and the details of algorithms are also presented.

Chapter 3 presents and analyzes the experimental results obtained. Interpretations and statistical analysis of repeated measures of resting EEG are also presented.

Chapter 4 discusses the limitations of this study.

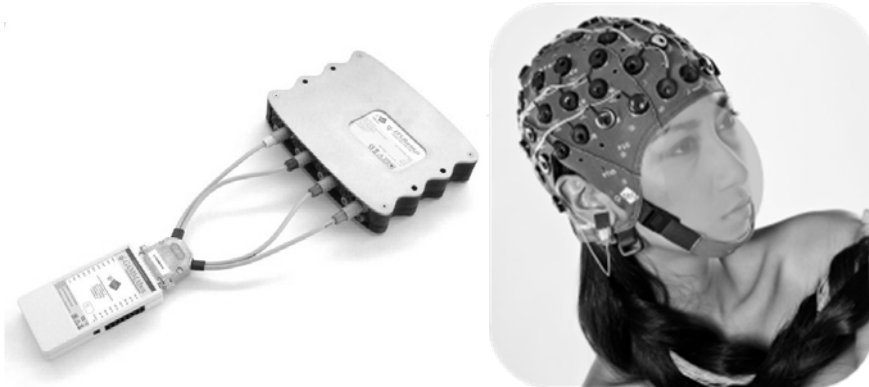
Chapter 5 summarizes the work carried out and concludes with an outline of future work.

CHAPTER 2. METHODS

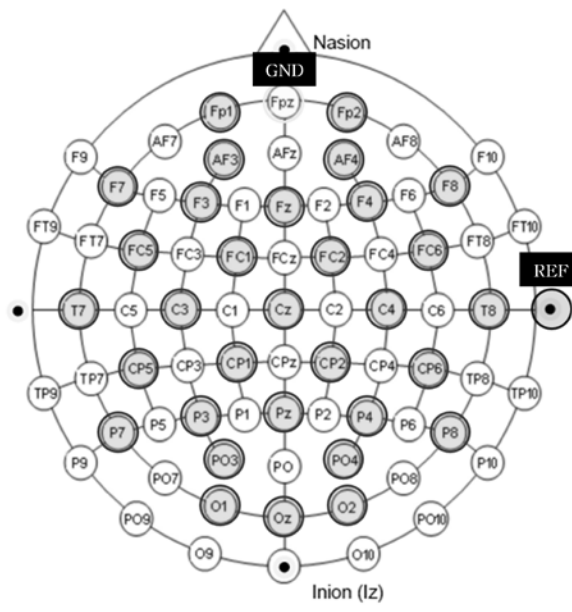
2.1 Electroencephalography measurement

This study included 20 healthy subjects without any mental illness. To simplify the measurement process, EEG was measured in the eyes-closed condition for 10 seconds using g.USBamp (g.tec, Austria). The EEG data were bandpass filtered in the frequency range 2–100 Hz and notch filtered at 60 Hz. A total of 32 electrodes were placed symmetrically on the scalp, as depicted in Figure 3, in accordance with the 10–20 international system. Considering the results of previous studies, the measurement sites covered ranged from the occipital region to the frontal region of the brain. A ground electrode was placed at Fpz and a reference electrode placed at the right ear. The EEG sampling rate was set to 600 Hz but was down-sampled to 100 Hz afterwards. In the measurement of EEG for clinical analysis, controlling external noise at strict levels is critical; however, in this thesis, the experiment was conducted under normal office

environmental conditions. In addition, the subjects were informed of the purpose and content of the experiments.



(a)



(b)

Figure 3. EEG measurement setup (a) (left) g.USBamp, (right) EEG cap on subject, (b) montage of 32 channels (10–20 system)

2.2 Experimental protocol

To evaluate the performance of the system for intra-variation of EEG, a minimum of 30 measurements, each comprising 10 seconds of continuous EEG, was taken for each subject on three different days. Thus, for each subject, a minimum of 90 measurements, each comprising 10 seconds of resting EEG, was obtained. The interval between measurements varied from a few days to a few weeks. Before measuring the EEG, conductive gel was smeared on the scalp at the point where each electrode was to be located. Recording was then conducted after checking the impedance status provided by the g.tec device and visually confirming the EEG signals displayed.

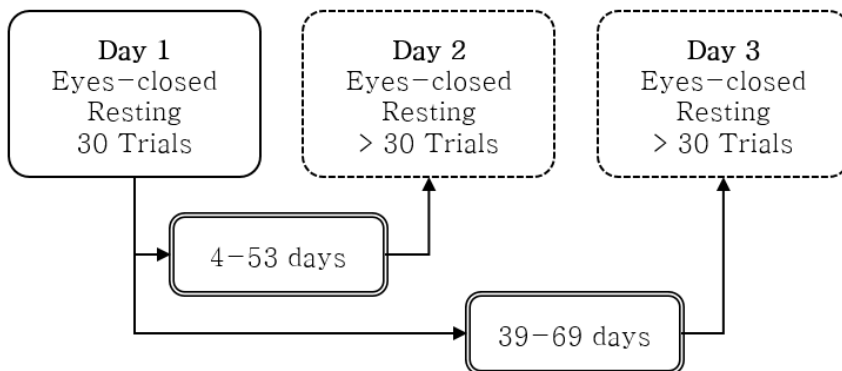


Figure 4. Measurement repetition interval

2.3 Design of the authentication system

The overall flow of the recognition system is illustrated in Figure 5. Artifact rejection and pre-processing of EEG occurs in the first step. This is followed by the feature extraction, classification, and performance evaluation steps. The details of each step are as follows.

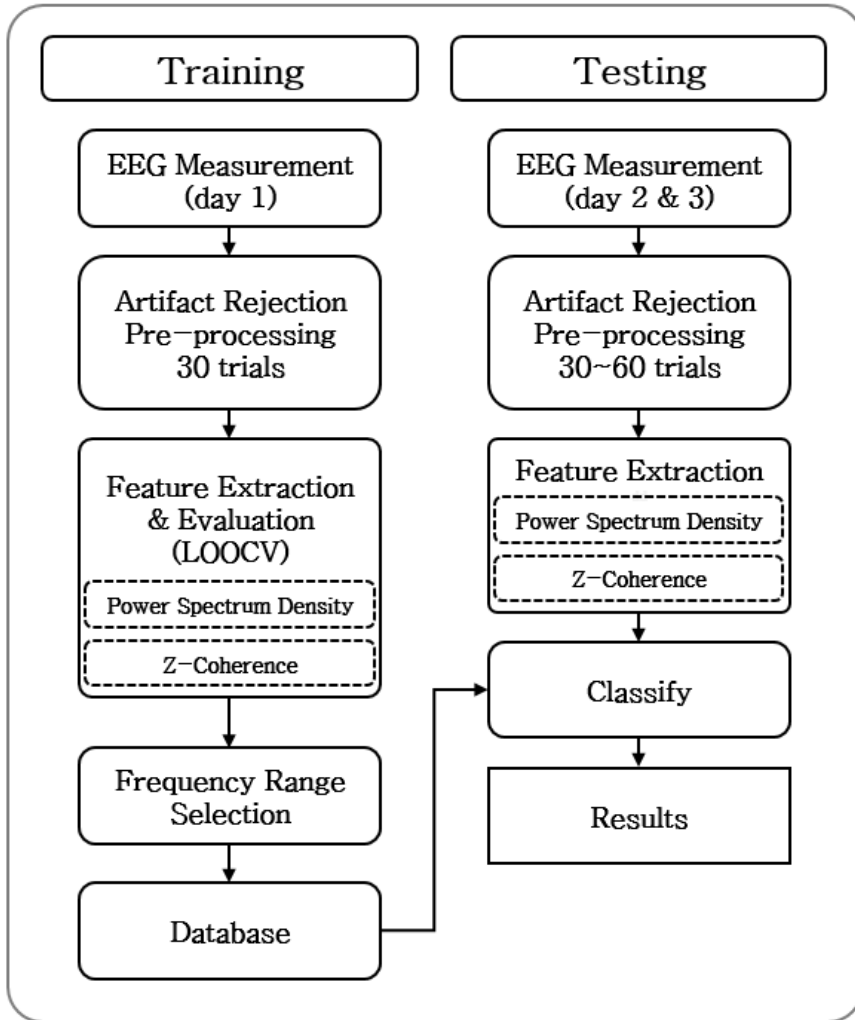


Figure 5. Flow of operations in the authentication system

2.3.1 Artifact rejection and signal pre-processing

The first step carried out by the recognition system is rejection of artifacts and pre-processing of EEG signals. Because EEG is very sensitive to external artifacts, the signals measured from the T7 and T8 sites were removed from the datasets owing to unstable contact by the corresponding electrodes. Consequently, only the EEG signals from a total of 30 channels were used. We considered continuous measurement of EEG for 10 seconds as one trial. During manual inspection of each trial, we rejected data that were considered to be affected by artifacts such as eye movement and facial muscle movements. There are several automatic methods that can be used to reject EEG artifacts affected by interference; however, a gold standard for badly measured EEG does not exist. Therefore, we chose to inspect them manually. Following rejection of severely contaminated trials, the remaining trials were down-sampled to 100 Hz and 45 Hz low-pass filtered to consider only the frequency range that covers delta (–4 Hz), theta (4–8 Hz), alpha (8–13 Hz), beta (13–30 Hz), and low gamma (30–40 Hz) rhythms of the brain.

EEG itself is a mix of neuronal signals from multiple local sources conducting through the volume. High-frequency components are significantly attenuated because of the high resistance of the skull; therefore, we did not expect to extract features from frequency components higher than 40 Hz.

2.3.2 Feature extraction

In order to recognize individuals, extraction of features that represent uniqueness is critical. In this study, we applied power spectrum density, which is widely used in previous studies, and coherence, which is the focus of recent research [19]. Details about each feature are given below and in Figure 6.

2.3.2.1 Power spectrum density

Power spectrum density represents the power of the signal distributed over the different frequencies. We extracted power spectrum density by computing the Welch's averaged modified periodogram. A sliding Hanning window of duration one second, with an overlap of 50% was applied to improve the estimation quality. The number of FFT points was set to 200 in order to have a PSD estimate with a frequency resolution of 0.5Hz. Setting the frequency of interest in the range of zero to 40 Hz resulted in one by 80 power spectrum feature vector for each

electrode (channel). When the eyes were closed, the alpha rhythm intensified.

2.3.2.2 Z-transformed Coherence

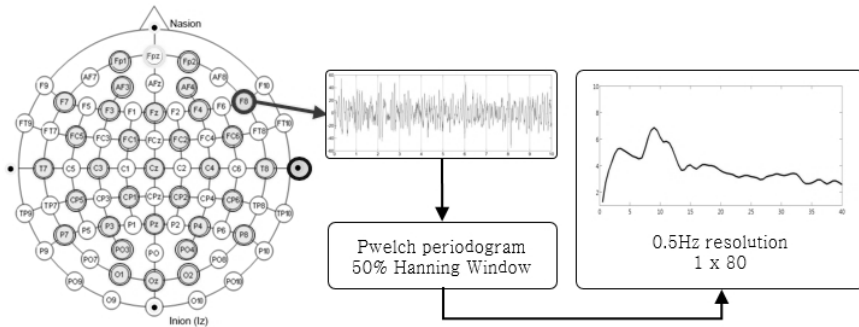
Spectral coherence represents the level of synchrony between two stationary signals at a specific frequency that in EEG, is interpreted as functional connectivity. In this study, we considered each electrode as a localized source and calculated cross-spectra, $S_{ij}(f)$. Spectral coherence is calculated as in equation (1).

$$COH_{ij}(f) = \frac{|S_{ij}(f)|^2}{S_{i,i}(f) \cdot S_{j,j}(f)} \dots\dots\dots (1)$$

Here, $S_{i,i}(f)$ and $S_{j,j}(f)$ are the respective auto-spectra computed by means of Welch's averaged modified periodogram, with the same parameters as used to compute PSD. After the calculations, the correlation of cross spectrum was transformed

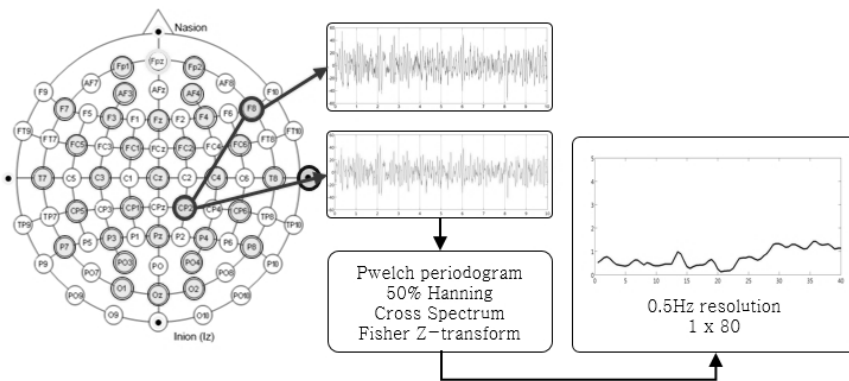
using Fisher's Z -transformation as in equation (2), in order to normalize the distributions [23].

$$z(f) = \frac{1}{2} \ln \left(\frac{1+r}{1-r} \right) = \tanh^{-1} r \dots\dots\dots (2)$$



N channels \rightarrow N PSD features

(a)



N channels \rightarrow $\frac{N}{2}C$ ZCOH features

(b)

Figure 6. Feature extraction from EEG signal: (a) Power spectrum density feature of each channel, (b) Z-transformed coherence of two channels

2.3.2.3 Feature evaluation of uniqueness

Before conducting testing with the EEG measured over subsequent days, we evaluated whether the extracted features represented the uniqueness of individuals by performing leave-one-out cross validation of the training data sets. Thirty measurements were taken from each subject; thus, for every leave-one-out cross validation, one out of 30 EEG datasets was used as the test dataset and the other 29 datasets used as training datasets. Classification was conducted using the k-nearest neighbor algorithm with Euclidean distance measures. Performance was measured by calculating the correct recognition rate in equation (3) from confusion matrix M.

$$\text{CRR} = \left(\frac{1}{N} \sum_1^N M[n,n]\right) \times 100 \dots\dots\dots (3)$$

2.3.2.4 Frequency range selection

Feature selection is as important as extraction of features because from a machine learning perspective, high dimension feature vectors do not always signify significant classification performance. In this sense, features can be partially selected by choosing the range of frequency. A partial frequency range comprising the spectrum of physiological EEG oscillations from delta (1–4 Hz), theta (4–8 Hz), alpha (8–13 Hz), beta (13–30 Hz), and low gamma (30–40 Hz) was selected. The performance was then evaluated for each EEG frequency range and combination of ranges. In addition, for each feature–PSD, ZCOH–performance was evaluated separately because of the numeric difference each provided. The number of PSD features is the same as the number of channels, whereas the number of ZCOH features is equal to the combination of channels, which is greater than the number of PSD features. Finally, in the testing process, the frequency range with the best performance in terms of uniqueness evaluation was selected.

2.3.3 Training and testing

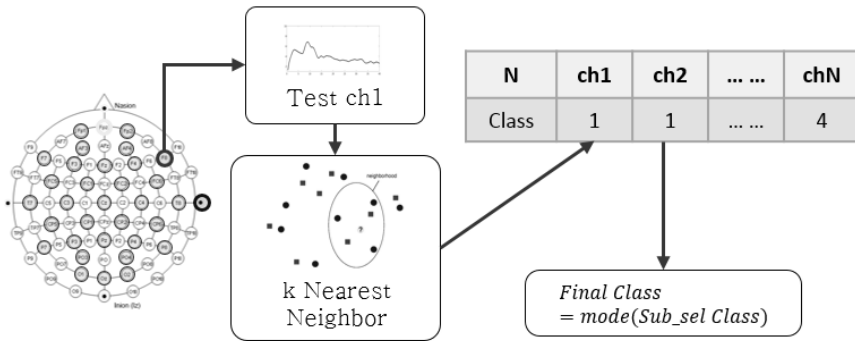
To compose the recognition system, training data are needed. In this study, 30 sets of repeatedly measured EEG data were utilized as training datasets and recognition performance was tested with EEG measured on different days from 20 subjects. Thus, a total of 600 EEG datasets were used as training datasets.

2.3.4 Classification

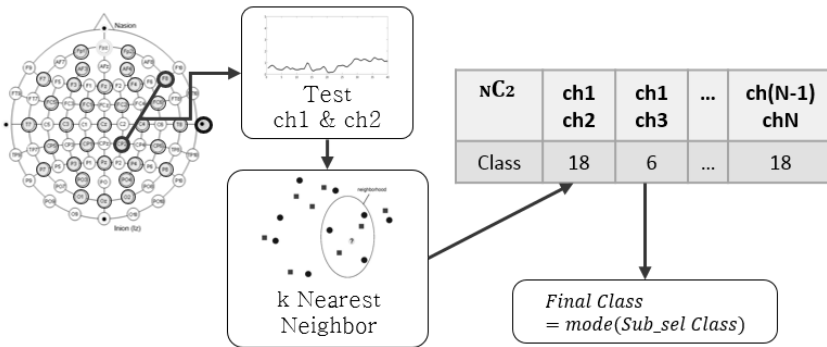
In this study, the decision as to the final class into which the test data are predicted was based on majority polling rules. For example, when using features to classify the test data, we applied the k-nearest neighbor algorithm to decide to which class the test data for each channels were closely related; for PSD this would be 30 times of polling. For the k-nearest neighbor algorithm, the parameters needed are the number of nearest neighbors and a method for measuring distance. We selected seven as the number of neighbors and utilized Euclidean distance. The final decision was obtained in accordance with equation (4):

$$\text{Class } S = \text{mode}(\text{Sub_Selected Classes of each ch / comb}) \dots\dots\dots (4)$$

Figure 7 illustrates the classification process.



(a)

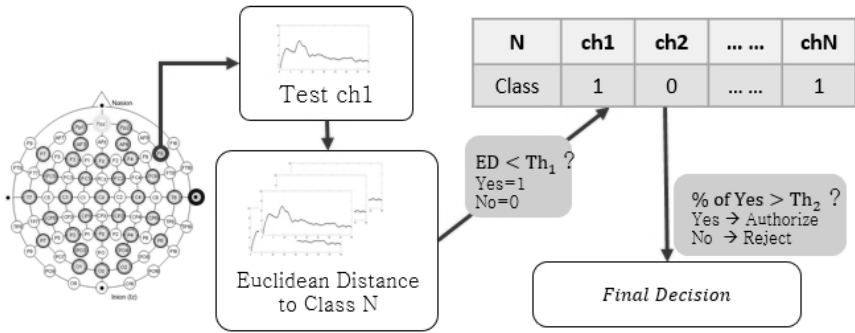


(b)

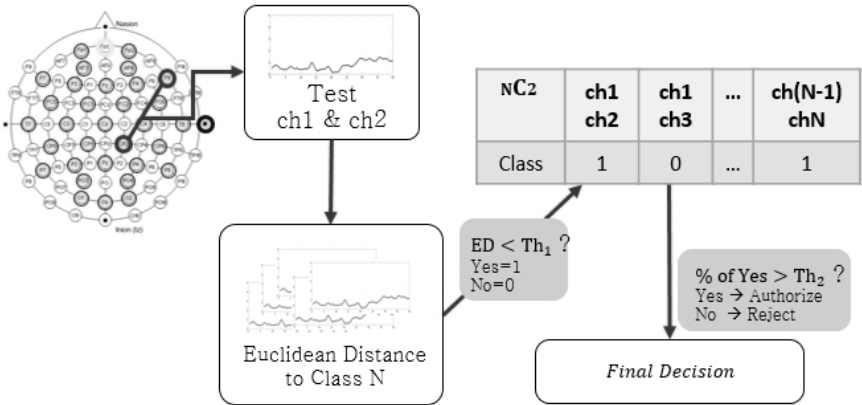
Figure 7. Classification method used in the “Registered only” mode: (a) Power spectrum density based, (b) Z-transformed coherence based

In addition to the classification process, either of two modes can be used to design the recognition system: the “Only registered” mode, which assumes that no one other than the subjects participating in the study is to be recognized, so that the system is only evaluated on how accurately it recognizes each subject; and the “Imposter”, in which the system not only tries to recognize each subject in the training dataset, but uses a set of criteria to decide whether to accept or reject it. The former mode does not require any additional criteria to determine whether the test data is very likely to match those in the training data. In contrast, the latter mode requires a threshold to determine whether the decision made is reasonable or not. In this study, the threshold was set to be the ratio of the frequency of the most selected classes to obtain the number of selections possible for each feature. The systematic flow of each mode is illustrated in Figure 8.

$$\text{Rejection decision } \left(\frac{\text{mode}(\text{Sub_Selected})}{\text{All Selection}} > \text{Threshold Ratio} \right) = \begin{cases} 1 \text{ accept and continue with recognition} \\ 0 \text{ reject and consider it an imposter} \end{cases} \dots\dots\dots (5)$$



(a)



(b)

Figure 8. Decision process in “Imposter” mode: (a) Power spectrum density based, (b) Z-transformed coherence based

2.3.5 Performance evaluation

Several performance evaluation metrics are used with recognition systems. These are presented in Table 2. The evaluation metrics can be selectively applied in accordance with how the recognition system is designed.

2.3.5.1 Registered only mode

Evaluations conducted of the system in “Registered only” mode are geared towards determining how accurately the test data are matched to their corresponding training dataset. Hence, the correct recognition rate for overall system evaluation is calculated and precision, recall, and F-score are calculated for each subject.

2.3.5.2 Imposter mode

In “Imposter” mode, the rejection criteria are set by selecting the threshold according to the rate of the majority polled. The system is evaluated by computing the false acceptance rate

(FAR), false rejection rate (FRR) and HTER with varying threshold levels. Setting a high threshold level results in a low false acceptance rate and an increased false rejection rate.

Table 2. Performance evaluation of the authentication system

| | Description | |
|-----------|---|---------------|
| CRR | Correct Recognition Rate | |
| FAR | False Acceptance Rate | |
| FRR | False Rejection Rate | |
| HTER | Half Total Error Rate | $(FAR+FRR)/2$ |
| EER | Equal Error Rate | |
| SE | Sensitivity | |
| SP | Specificity | |
| Precision | $TP / (TP + FP)$ | |
| Recall | $TP / (TP + FN)$ | |
| F-score | $2 \cdot \frac{\text{Precision} \cdot \text{Recall}}{\text{Precision} + \text{Recall}}$ | |

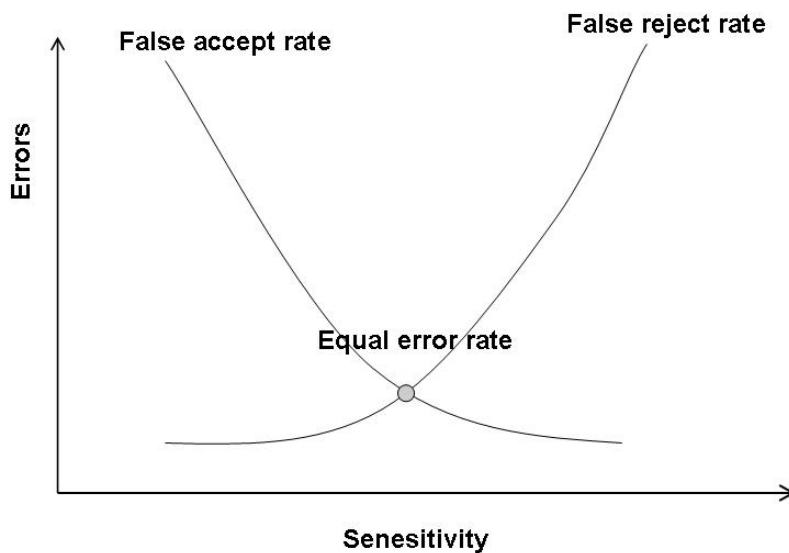


Figure 9. Description of false acceptance rate and false reject rate with level of sensitivity

2.4 Stability evaluation statistics

The major factor that affects accuracy of recognition is intra- variations in EEG measured in different physiological and psychological conditions. Following recognition of performance, test-retest reliability was performed on the features extracted from the EEGs collected over all three days. With the assumption that frequency rhythms are independent, an ANOVA test was performed and features that are significantly reliable and highly correlated for each individual as representing uniqueness were filtered. The process is outlined in Figure 10.

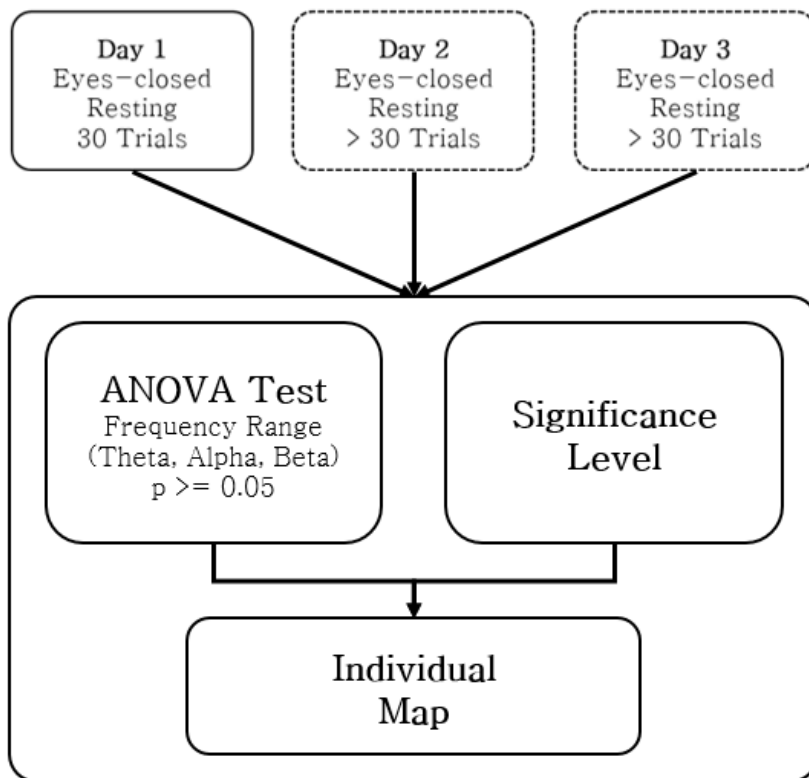


Figure 10. Process description of statistical test.

CHAPTER 3. RESULTS

3.1 Details of materials used

A total of 20 healthy adult subjects (fifteen males, five females, and average age 27.95 years) participated in this study (given in Table 3). All the participants were in normal condition; i.e., no sleep deprivation, no excessive intake of caffeine, and not highly aroused. The EEGs of all but one subject (S18) were measured over three separate days. The average interval between the first and second days was 22.9 days and 46.8 days between the first and third days.

Table 3. General information pertaining to the subjects who participated and the interval (days) of measurements

| Subject | Gender | Age | Int#1-2 | Int#1-3 |
|---------|--------|------|---------|---------|
| S01 | M | 32 | 21 | 48 |
| S02 | M | 31 | 28 | 46 |
| S03 | M | 25 | 27 | 40 |
| S04 | M | 31 | 13 | 61 |
| S05 | F | 23 | 9 | 47 |
| S06 | M | 28 | 26 | 46 |
| S07 | M | 29 | 50 | 69 |
| S08 | M | 23 | 7 | 45 |
| S09 | M | 28 | 28 | 42 |
| S10 | M | 32 | 14 | 45 |
| S11 | F | 28 | 21 | 39 |
| S12 | M | 28 | 30 | 41 |
| S13 | F | 33 | 21 | 40 |
| S14 | F | 26 | 4 | 32 |
| S15 | M | 24 | 18 | 65 |
| S16 | M | 24 | 18 | 40 |
| S17 | F | 26 | 63 | 56 |
| S18 | M | 29 | 14 | N/A |
| S19 | M | 29 | 23 | 42 |
| S20 | M | 30 | 33 | 46 |
| Mean | | 27.9 | 22.9 | 46.8 |
| Std. | | 3.0 | 12.5 | 9.5 |

Although the experiment was conducted by confirming the raw EEG signals presented in real time, several trials were contaminated either by micro-movement of eyes during the eyes-closed state or facial muscle movements. For this reason, channels T7 and T8 were eliminated and only the 30 remaining channels were used in the final tests. Trials were rejected on the basis of two criteria: The first was that we regarded signals that had maximum power at frequencies less than 4 Hz as the effect of eye movements. The second was that we regarded any signal that had overall high power over all the frequency range (-40 Hz) as the effect of facial muscle movement considering that electromyography occurs within the frequency range 20-400 Hz. Examples of rejected signals are presented in Figure 11. Following the rejection, the total number of trials used in testing for each subject varied, as shown in Table 4.

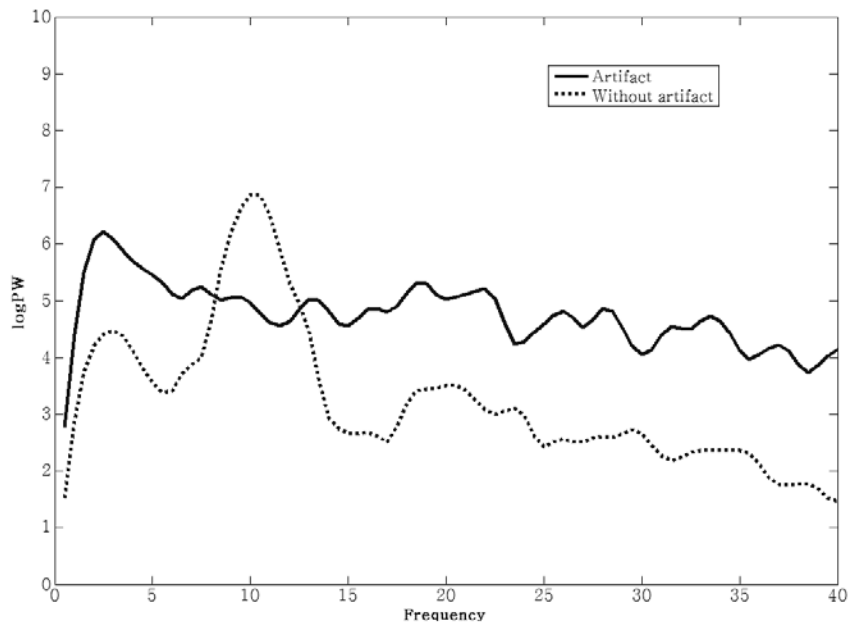


Figure 11. Example PSD of rejected trial and regular trial

Table 4. Number of trials used in the tests for each subject.

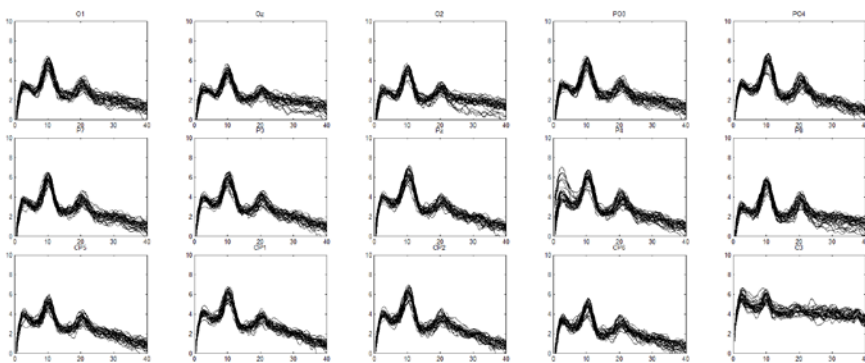
| Subject | # Trials | Subject | # Trials |
|---------|----------|--------------|--------------|
| S01 | 60 | S11 | 60 |
| S02 | 60 | S12 | 60 |
| S03 | 60 | S13 | 48 |
| S04 | 96 | S14 | 30* |
| S05 | 66 | S15 | 93 |
| S06 | 60 | S16 | 60 |
| S07 | 60 | S17 | 60 |
| S08 | 30* | S18 | 30** |
| S09 | 60 | S19 | 60 |
| S10 | 90 | S20 | 30* |
| | | Total | 1,173 |

3.2 Feature vectors and evaluation

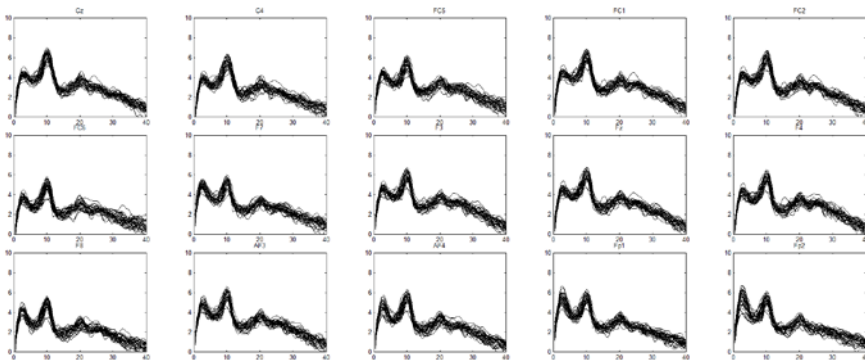
After the rejection of artifacts, power spectrum density and Z -coherence features were extracted from the 30 trials measured on the first day for the training dataset and on other days for the testing dataset.

3.2.1 Power spectrum density

In Figure 12, the PSD features of 30 channels, repeatedly measured 30 times, for one subject are presented. In Figure 13, the PSD features of a single channel for each of the subjects are presented. By carefully inspecting Figure 13, it can be intuitively determined that the power spectrum density characteristics of each subject differed.



(a)



(b)

Figure 12. PSD feature plots of training data: S09 (a) 1–15 channels (Occipital & Parietal), (b) 16–30 channels (Central & Frontal)

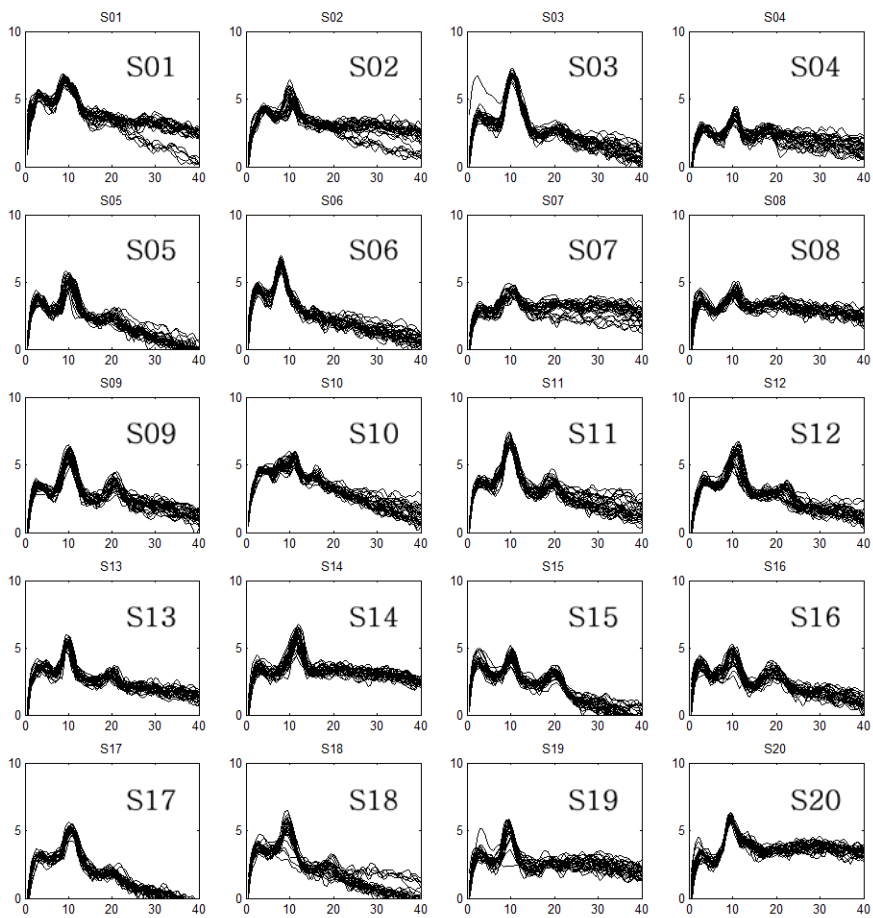


Figure 13. PSD plot of a single channel (O1) for each of the 20 subjects

3.2.2 Z-transformed coherence

In Figure 14, the ZCOH features measured 30 times for a single subject is presented. Because the number of channels utilized is 30, the total combination of ZCOH is 435. For comparison between subjects, plots of the ZCOH for each single combination are presented in Figure 15. The ZCOH reflects relatively less

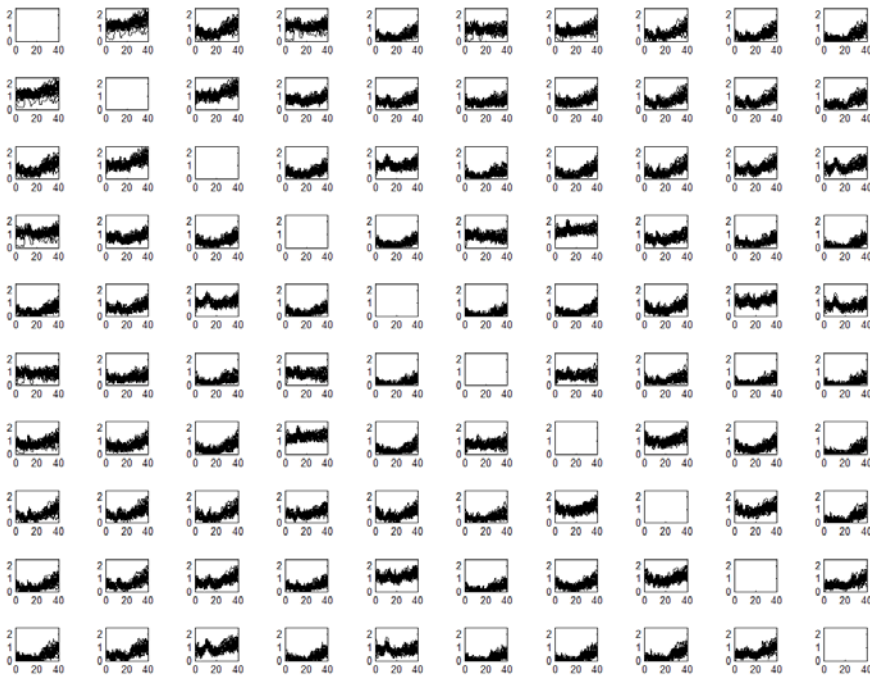


Figure 14. Z-coherence plot of the training data for a single subject. Combinations of ch1 to ch10

distinct characteristics than PSD; however, it provides more features.

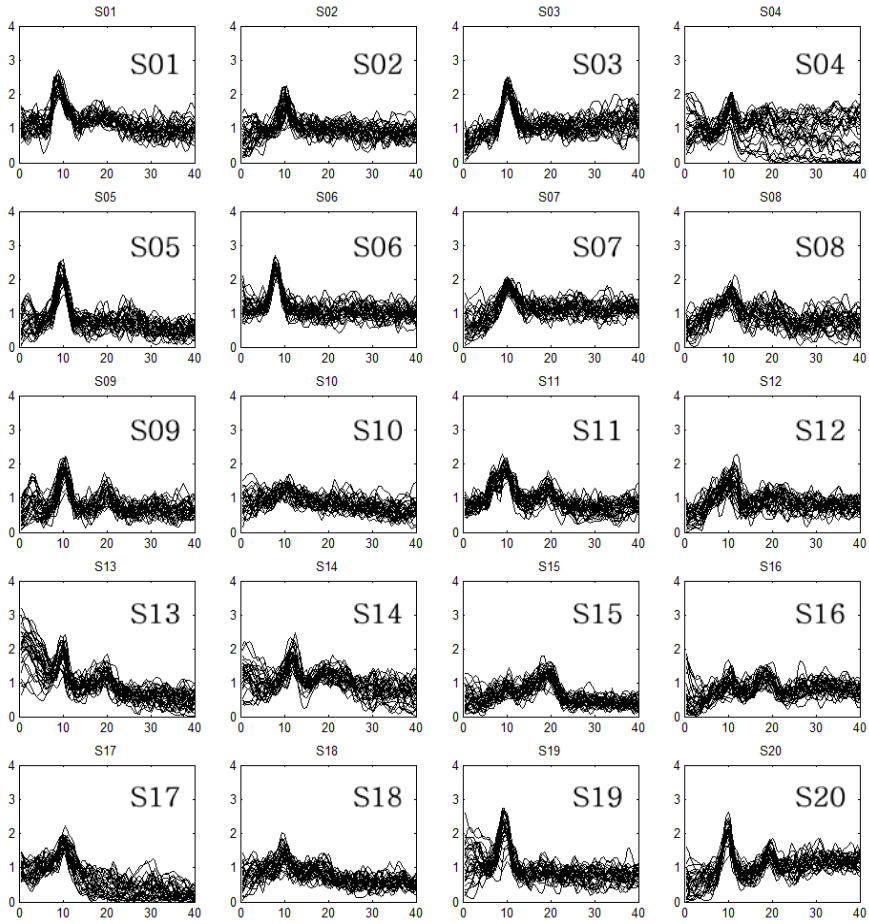


Figure 15. ZCOH plot of a single combination (Fp1 & Fp2) for each of the 20 subjects

3.2.3 Uniqueness evaluation (LOOCV)

To evaluate whether the PSD and ZCOH represented the uniqueness of the individuals, we conducted leave-one-out cross validation on the training set.

3.2.3.1 Result of power spectrum density

The number of training datasets for each subject was 30. Thus, a total of 600 leave-one-out cross validations was conducted. The performance result in terms of correct recognition rate is presented in Figures 16 and 17 with different frequency ranges applied. In the classification process, parameter k , which signifies the number of neighbors to consider in the decision-making process, could be manually controlled. In our study, parameter k was set to 1, 5, 7, 10, and 20. A maximum correct recognition rate of 98.83% was achieved with $k = 1$, at a frequency range of 1–40 Hz.

Table 5. PSD LOOCV CRR with different frequency ranges and varying k-values.

| | Parameter k | | | | |
|----------------------------------|--------------|-------|-------|-------|-------|
| | 1 | 5 | 7 | 10 | 20 |
| 1-4 Hz δ | 42.83 | 40.67 | 43.50 | 41.17 | 43.50 |
| 4-8 Hz θ | 65.17 | 61.17 | 62.83 | 62.33 | 61.50 |
| 8-13 Hz α | 81.67 | 80.00 | 78.50 | 77.00 | 75.17 |
| 13-30 Hz β | 89.33 | 87.67 | 88.00 | 89.50 | 87.00 |
| 4-13 Hz $\theta \alpha$ | 90.83 | 88.00 | 87.00 | 86.33 | 85.50 |
| 8-30 Hz $\alpha \beta$ | 96.67 | 96.00 | 95.50 | 94.83 | 94.17 |
| 4-30 Hz $\theta \alpha \beta$ | 98.17 | 97.17 | 96.83 | 96.33 | 95.50 |
| 1-40 Hz all | 98.83 | 97.00 | 97.67 | 97.33 | 96.33 |

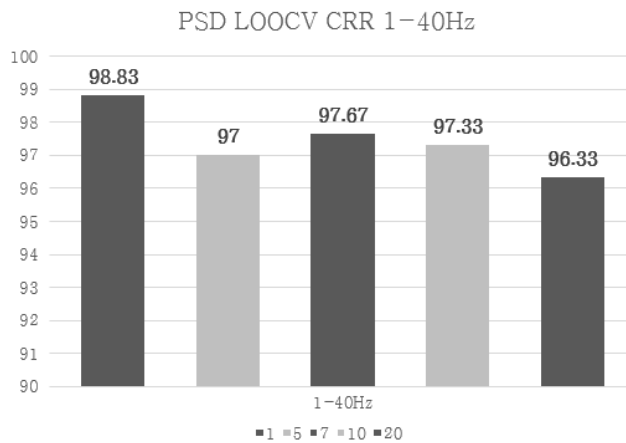


Figure 16. PSD: Correct recognition rate with fixed frequency range and varying k-values.

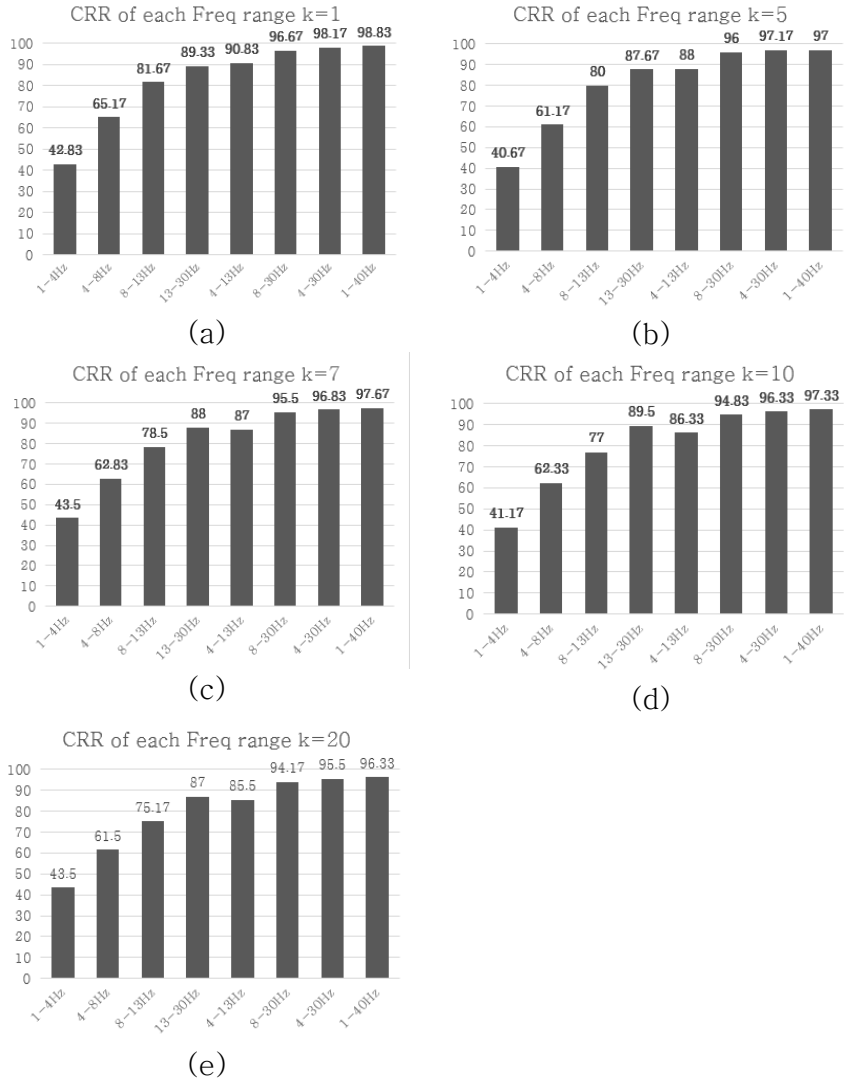


Figure 17. PSD: Correct recognition rate for all frequency ranges and k -values. (a) $k = 1$, (b) $k = 5$, (c) $k = 7$, (d) $k = 10$ and (e) $k = 20$.

3.2.3.2 Result of Z-transformed coherence

The number of training datasets for each subject was the same as PSD. The resulting performance in terms of correct recognition rate is presented in Figure 18. Figure 19, with different frequency ranges applied and variation of parameter k , is the same as the PSD feature. A maximum correct recognition rate of 99.67% was achieved with $k = 1$, at a frequency range of 1–40 Hz.

3.2.3.3 Frequency range selection

From the results of leave-one-out cross validation previously presented, the recognition performance of each individual was best when using a frequency range of one to 40 Hz with PSD (98.83%) and ZCOH (99.67%). Therefore, the 1–40 Hz frequency range was finally selected in recognizing the test data measured on different days.

Table 6. ZCOH LOOCV CRR with different frequency ranges and varying k values.

| | Parameter k | | | | |
|-----------------------|-------------|-------|-------|-------|-------|
| | 1 | 5 | 7 | 10 | 20 |
| 1-4Hz | 64.17 | 38.50 | 48.17 | 52.50 | 53.00 |
| δ | | | | | |
| 4-8Hz | 80.00 | 56.00 | 66.00 | 68.00 | 71.83 |
| θ | | | | | |
| 8-13Hz | 88.00 | 80.83 | 82.33 | 83.17 | 82.33 |
| α | | | | | |
| 13-30Hz | 94.67 | 86.67 | 88.33 | 89.33 | 89.17 |
| β | | | | | |
| 4-13Hz | 95.00 | 91.17 | 94.33 | 98.83 | 92.17 |
| $\theta \alpha$ | | | | | |
| 8-30Hz | 98.83 | 97.33 | 97.50 | 97.17 | 96.83 |
| $\alpha \beta$ | | | | | |
| 4-30Hz | 99.67 | 99.00 | 99.67 | 99.17 | 98.17 |
| $\theta \alpha \beta$ | | | | | |
| 1-40Hz | 99.67 | 99.00 | 98.67 | 98.50 | 97.50 |
| all | | | | | |

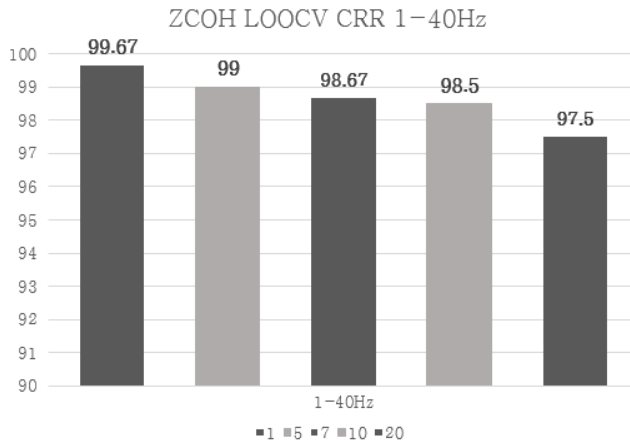


Figure 18. ZCOH: Correct recognition rate (%) with fixed frequency range and varying value

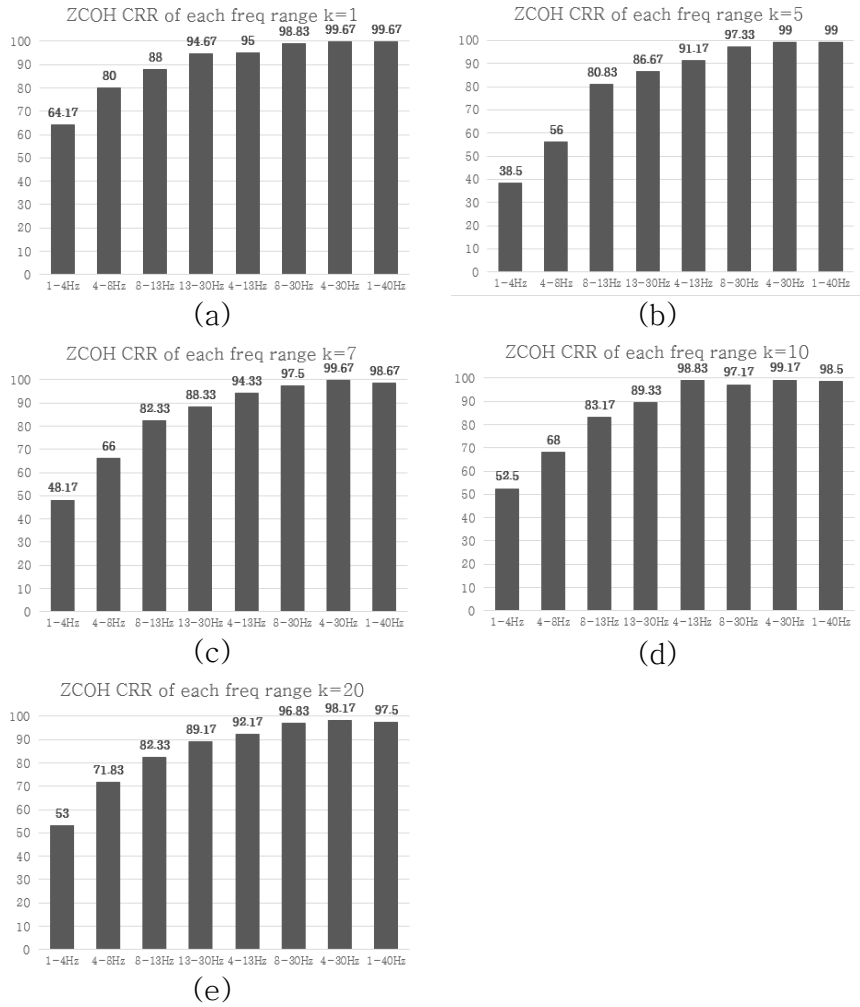


Figure 19. ZCOH: Correct recognition rate for all frequency ranges and k -values. (a) $k = 1$, (b) $k = 5$, (c) $k = 7$, (d) $k = 10$, and (e) $k = 20$.

3.3 Authentication test evaluation

As previously mentioned in section 2.3.5, different performance evaluations can be applied to the two modes. For the “Only registered” mode, correct recognition rate was calculated for overall performance, with precision, recall, specificity, and F-score calculated for individual performance. For the “Imposter” mode, we computed false acceptance rate (FAR), false rejection rate (FRR), and half of total error rate (HTER) with varying threshold levels. The results are shown with the best correct recognition rate relative parameter k .

3.3.1 Registered only mode

The “Registered only” mode assumes that recognition should only be attempted for registered users in the test. The performance was evaluated with the fixed frequency range (1–40 Hz) previously selected and parameter k at 1, 5, 7, 10, and 20. The best results obtained are presented below.

3.3.1.1 Power spectrum density

Testing a total of 1,173 datasets measured on different days by using the power spectrum features resulted in the best correct recognition rate of 80.39% with an average of 81.35% for precision, 78.02% for recall, 99.04% for specificity, and 0.78 for F-score. The performance of each subject is presented in Table 7.

3.3.1.2 Z-transformed coherence

In the results obtained using the Z-coherence features, the best correct recognition rate of 75.70% was achieved with an average 80.04% for precision, 74.88% for recall, 99.81% for specificity, and 0.75 for F-score, with $k = 7$. The performance of each subject is presented in Table 8.

Table 7. Identification performance of test data for each subjects using PSD (1–40 Hz).

| K= 5 (CRR 80.39%) | | | | |
|-------------------|--------------|--------------|--------------|-------------|
| Subject | Precision | Recall | Specificity | F-score |
| S01 | 94.73 | 90.00 | 99.50 | 0.92 |
| S02 | 43.00 | 71.66 | 98.53 | 0.54 |
| S03 | 93.65 | 98.33 | 99.91 | 0.96 |
| S04 | 88.77 | 90.62 | 99.27 | 0.90 |
| S05 | 83.33 | 45.45 | 96.99 | 0.59 |
| S06 | 100.00 | 91.66 | 99.59 | 0.96 |
| S07 | 76.11 | 85.00 | 99.25 | 0.80 |
| S08 | 48.57 | 56.66 | 98.89 | 0.52 |
| S09 | 92.85 | 65.00 | 98.26 | 0.76 |
| S10 | 100.00 | 91.11 | 99.36 | 0.95 |
| S11 | 73.07 | 95.00 | 99.75 | 0.83 |
| S12 | 93.10 | 90.00 | 99.50 | 0.92 |
| S13 | 90.62 | 60.41 | 98.41 | 0.73 |
| S14 | 90.62 | 96.66 | 99.91 | 0.94 |
| S15 | 97.61 | 88.17 | 99.12 | 0.93 |
| S16 | 72.41 | 70.00 | 98.49 | 0.71 |
| S17 | 66.23 | 85.00 | 99.24 | 0.74 |
| S18 | 49.09 | 90.00 | 99.74 | 0.64 |
| S19 | 85.71 | 80.00 | 99.01 | 0.83 |
| S20 | 87.50 | 23.33 | 98.04 | 0.37 |
| Avg | 81.35 | 78.20 | 99.04 | 0.78 |

Table 8. Identification performance of test data for each subjects using ZCOH (1–40 Hz).

| K= 7 (CRR 75.70%) | | | | |
|-------------------|--------------|--------------|--------------|-------------|
| Subject | Precision | Recall | Specificity | F-score |
| S01 | 69.56 | 80.00 | 99.00 | 0.74 |
| S02 | 90.69 | 65.00 | 98.26 | 0.76 |
| S03 | 62.92 | 93.33 | 99.66 | 0.75 |
| S04 | 72.82 | 69.79 | 97.61 | 0.71 |
| S05 | 89.28 | 75.75 | 96.68 | 0.82 |
| S06 | 98.18 | 90.00 | 99.51 | 0.94 |
| S07 | 58.82 | 83.33 | 99.15 | 0.69 |
| S08 | 42.85 | 20.00 | 97.95 | 0.27 |
| S09 | 94.44 | 56.66 | 97.84 | 0.71 |
| S10 | 89.65 | 86.66 | 99.03 | 0.88 |
| S11 | 84.84 | 93.33 | 99.67 | 0.89 |
| S12 | 86.66 | 86.66 | 99.34 | 0.87 |
| S13 | 83.78 | 64.58 | 98.58 | 0.73 |
| S14 | 88.46 | 76.66 | 99.41 | 0.82 |
| S15 | 86.25 | 74.19 | 98.05 | 0.80 |
| S16 | 83.33 | 75.00 | 98.75 | 0.79 |
| S17 | 97.95 | 80.00 | 99.01 | 0.88 |
| S18 | 20.51 | 80.00 | 99.45 | 0.33 |
| S19 | 100.00 | 46.66 | 97.33 | 0.64 |
| S20 | 100.00 | 100.00 | 100.00 | 100.00 |
| Avg | 80.04 | 74.88 | 98.81 | 0.75 |

3.3.2 Imposter mode

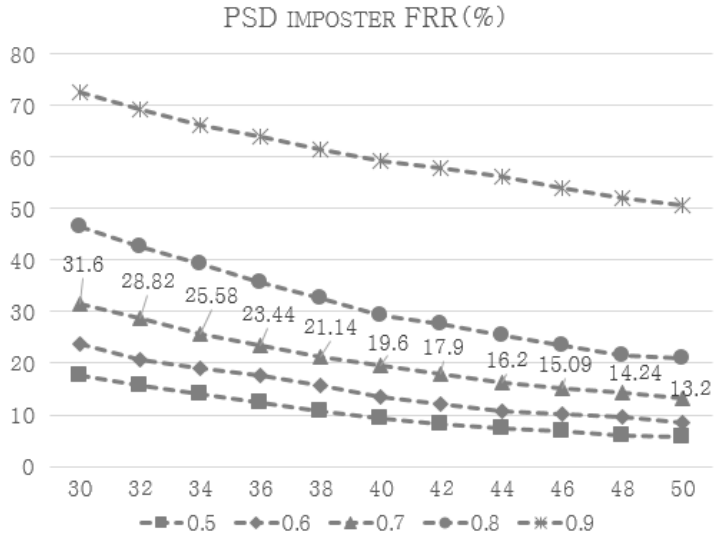
The “Imposter” mode was utilized to evaluate the recognition rate by setting the absolute threshold on the Euclidean distance measure to reject improper authentication. Because the decision is made based on whether the test data relatively matches the corresponding trained data by measuring the Euclidean distance, we empirically applied several threshold values. Furthermore, the testing process is slightly different from that of the “Registered Only” mode. Thus, we assumed the possibility that person A would try to authenticate on person B’s data. In this sense, every test dataset is assumed to have been the target of access attempts by every subject. As a result, a total of 23,460 testing trials was conducted. Evaluation of this mode was performed by calculating FAR, FRR, and HTER.

3.3.2.1 Power spectrum density

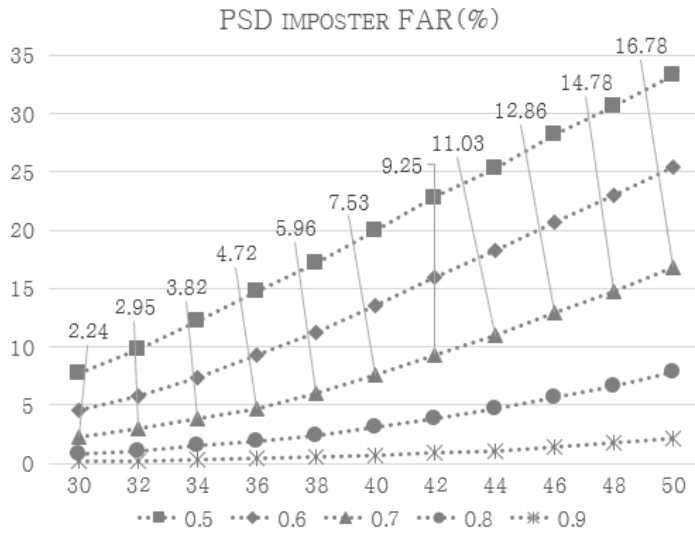
For power spectrum density, we empirically applied Euclidean distance threshold values from 30 to 50 in increments of 2. Each channel was checked to determine whether the Euclidean distance was below the threshold value and the ratio of channels that surpassed the threshold all the possible channels, respectively 30, logically counted. Then, the ratio itself was checked to determine whether it exceeded the minimum level for deciding whether to accept or reject. FAR and FRR with varying Euclidean distance threshold and varying proportion threshold are presented in Table 9 and Figure 20. HTER is presented in Figure 21.

Table 9. Imposter mode: FRR and FAR of test data using PSD (1–40 Hz) with varying thresholds.

| Ratio threshold of passed channels to total number of channels | | | | | | | | | | |
|--|------|------|------|------|------|------|------|------|------|------|
| | 50% | | 60% | | 70% | | 80% | | 90% | |
| ED | FAR | FRR |
| 30 | 7.74 | 17.6 | 4.52 | 23.6 | 2.24 | 31.6 | 0.79 | 46.4 | 0.21 | 72.4 |
| 32 | 9.73 | 15.8 | 5.77 | 20.8 | 2.95 | 28.8 | 1.06 | 42.5 | 0.25 | 69.1 |
| 34 | 12.2 | 13.9 | 7.37 | 19.0 | 3.82 | 25.6 | 1.47 | 39.2 | 0.35 | 66.1 |
| 36 | 14.7 | 12.3 | 9.24 | 17.7 | 4.72 | 23.4 | 1.90 | 35.6 | 0.45 | 63.9 |
| 38 | 17.2 | 10.8 | 11.3 | 15.6 | 5.96 | 21.1 | 2.42 | 32.7 | 0.57 | 61.3 |
| 40 | 20.0 | 9.38 | 13.5 | 13.6 | 7.53 | 19.6 | 3.11 | 29.4 | 0.69 | 59.2 |
| 42 | 22.8 | 8.35 | 15.9 | 12.0 | 9.25 | 17.9 | 3.85 | 27.5 | 0.87 | 57.7 |
| 44 | 25.3 | 7.50 | 18.2 | 10.8 | 11.0 | 16.2 | 4.64 | 25.3 | 1.08 | 56.1 |
| 46 | 28.2 | 6.73 | 20.7 | 10.1 | 12.9 | 15.1 | 5.62 | 23.4 | 1.44 | 54.1 |
| 48 | 30.7 | 6.14 | 23.0 | 9.55 | 14.8 | 14.2 | 6.58 | 21.7 | 1.82 | 52.1 |
| 50 | 33.2 | 5.80 | 25.4 | 8.60 | 16.8 | 13.2 | 7.80 | 21.0 | 2.13 | 50.6 |



(a)



(b)

Figure 20. PSD Imposter: (a) false rejection rate, (b) false acceptance rate plot (Labeled is at threshold 0.7)

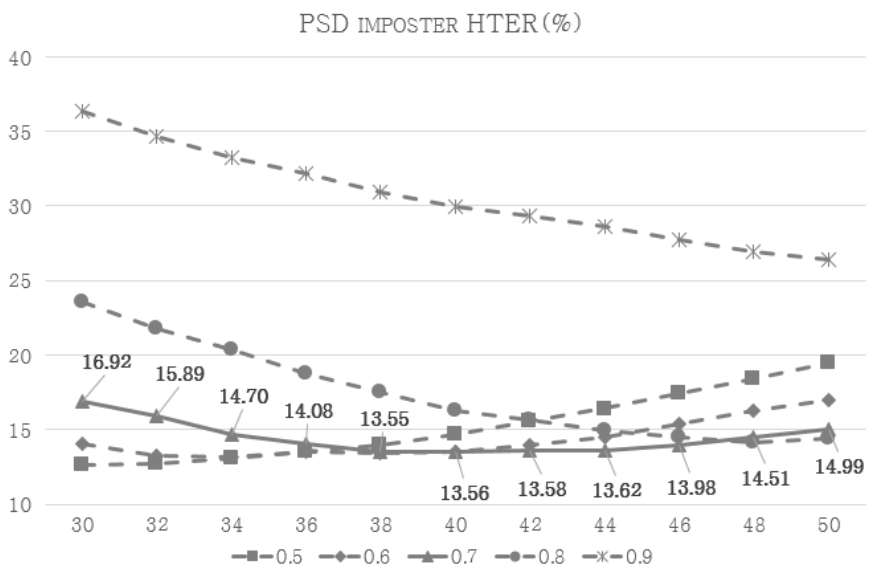


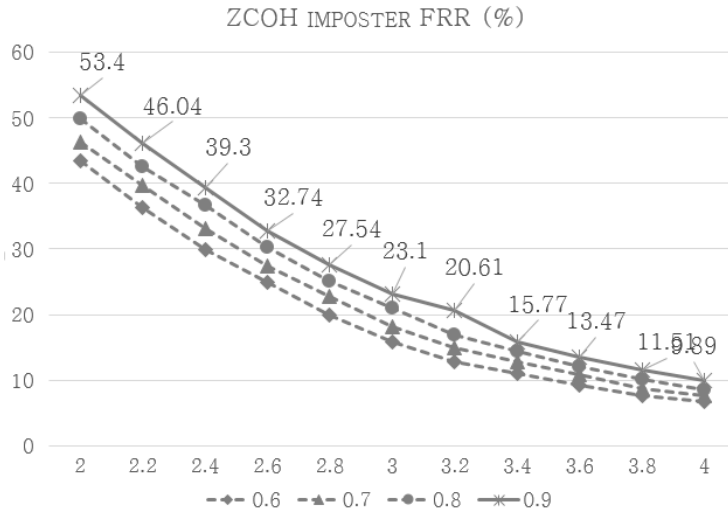
Figure 21. PSD Imposter: Half total error rate (Labeled is at threshold 0.7)

3.3.2.2 Z-transformed coherence

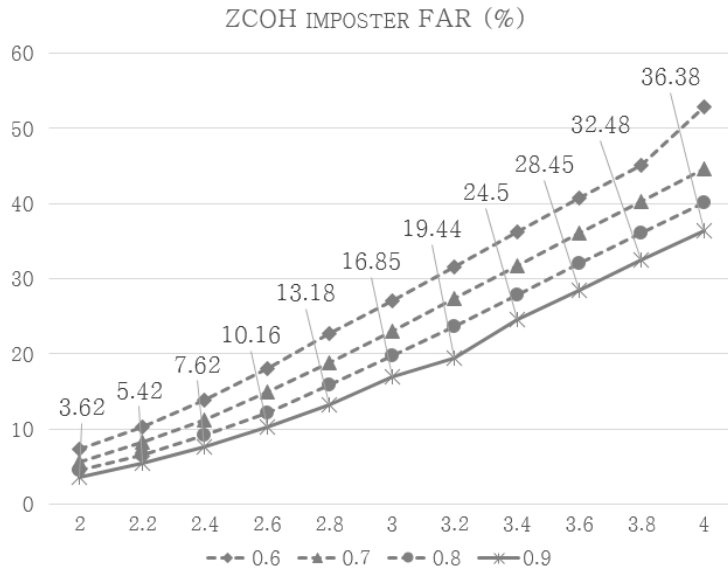
In the evaluation by ZCOH, the same method of selecting the threshold PSD was applied. The threshold value was empirically selected, from 2 to 4 in 0.2 increments. Each combination checked whether the Euclidean distance was below the threshold value and logically counted the ratio of combinations that surpassed the threshold to the total possible combinations, respectively 435. Then, the ratio itself was checked to determine whether it exceeded the minimum level in order to decide whether to accept or reject. FAR and FRR with varying Euclidean distance thresholds and varying proportion thresholds are presented in Table 10 and Figure 22. HTER is presented in Figure 23.

Table 10. Imposter mode: FRR and FAR of test data using ZCOH (1–40 Hz) with varying thresholds.

| Ratio threshold of passed combinations to total number of combinations | | | | | | | | |
|--|------|------|------|------|------|------|------|------|
| | 60% | | 70% | | 80% | | 90% | |
| ED | FAR | FRR | FAR | FRR | FAR | FRR | FAR | FRR |
| 2.0 | 6.21 | 43.3 | 4.81 | 46.3 | 3.79 | 49.7 | 2.31 | 53.5 |
| 2.2 | 8.71 | 36.2 | 6.99 | 39.6 | 5.59 | 42.5 | 3.47 | 46.0 |
| 2.4 | 11.7 | 29.8 | 9.43 | 33.2 | 7.77 | 36.6 | 4.90 | 39.3 |
| 2.6 | 15.3 | 25.0 | 12.6 | 27.5 | 10.3 | 30.2 | 6.58 | 32.7 |
| 2.8 | 18.9 | 19.9 | 15.9 | 22.7 | 13.4 | 25.1 | 8.59 | 27.5 |
| 3.0 | 22.8 | 15.8 | 19.4 | 18.1 | 16.6 | 21.0 | 11.0 | 23.1 |
| 3.2 | 26.7 | 12.9 | 23.1 | 14.9 | 20.0 | 17.0 | 17.4 | 19.4 |
| 3.4 | 30.7 | 11.1 | 26.9 | 12.9 | 23.5 | 14.4 | 20.7 | 15.8 |
| 3.6 | 34.6 | 9.21 | 30.5 | 10.8 | 27.1 | 12.1 | 24.0 | 13.5 |
| 3.8 | 38.5 | 7.59 | 34.3 | 8.78 | 30.6 | 10.1 | 27.4 | 11.5 |
| 4.0 | 42.3 | 6.82 | 38.1 | 7.59 | 34.2 | 8.53 | 30.8 | 9.89 |



(a)



(b)

Figure 22. ZCOH Imposter: (a) false rejection rate, (b) false acceptance rate plot (Label is at threshold 0.9)

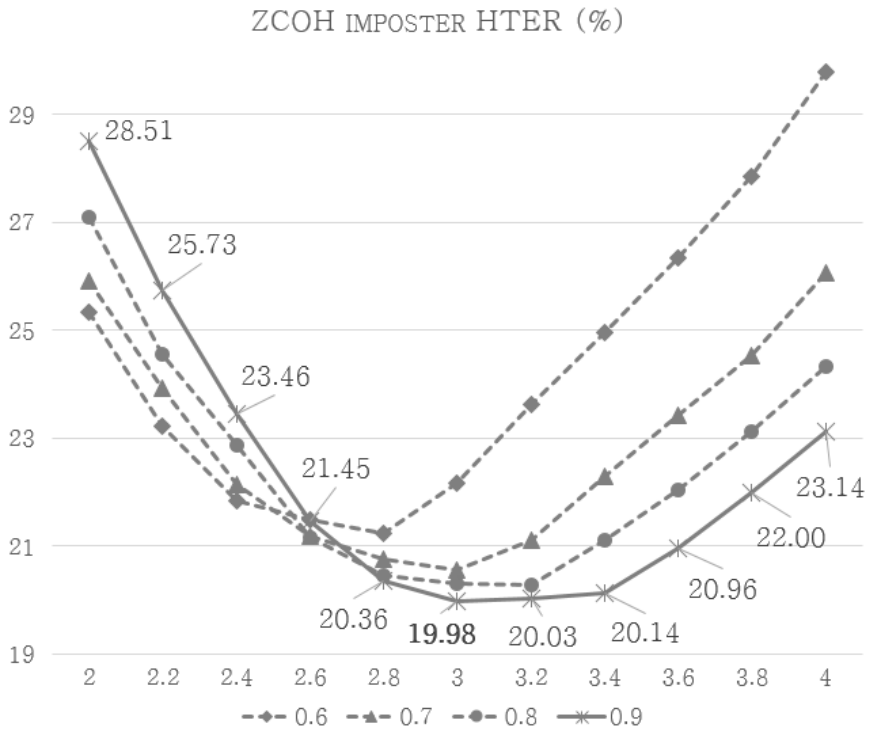


Figure 23. ZCOH Imposter: Half of total error rate (Labeled is at threshold 0.9)

3.4 Stability evaluation statistics

The major factor that affects performance of recognition is intra-variation of the EEG measured in different physiological and psychological conditions. It was found in a study conducted by Kondacs et al. that features of PSD are stable over time, as long as 62 months however, coherence has not been examined in previous studies [20]. In addition, we concluded from the results of the “Imposter mode” that not all ZCOH combinations contain significant information, even though ZCOH does reflect distinct characteristics.

In order to determine which combinations are significant for each subject and determine its stability over time, test-retest reliability was performed on ZCOH extracted from EEG collected on all three days. With the assumption that frequency rhythms are independent, analysis of variance (ANOVA) test was performed and ZCOH features that are significant and stable over time for each subject to represent uniqueness were filtered. Because some trials were rejected, the statistics for subjects 14 and 18 were excluded.

3.4.1 Significant Z-coherence of individuals

Significant and stable coherence maps for each individual are presented in Figures 24, 25, and 26 with respect to the frequency bands for theta, alpha, and beta along with the result of ANOVA test that reflected no difference in the measurements for the three days and a high correlation value. A total of 13 channels were analyzed as the artifact free channels for all subjects measured on all days. These are colored in the topography. Although we did not filter the ZCOH in the training process, using significant combinations that are stable over time and high in correlation for each subject can be applied as a feature filtering process.

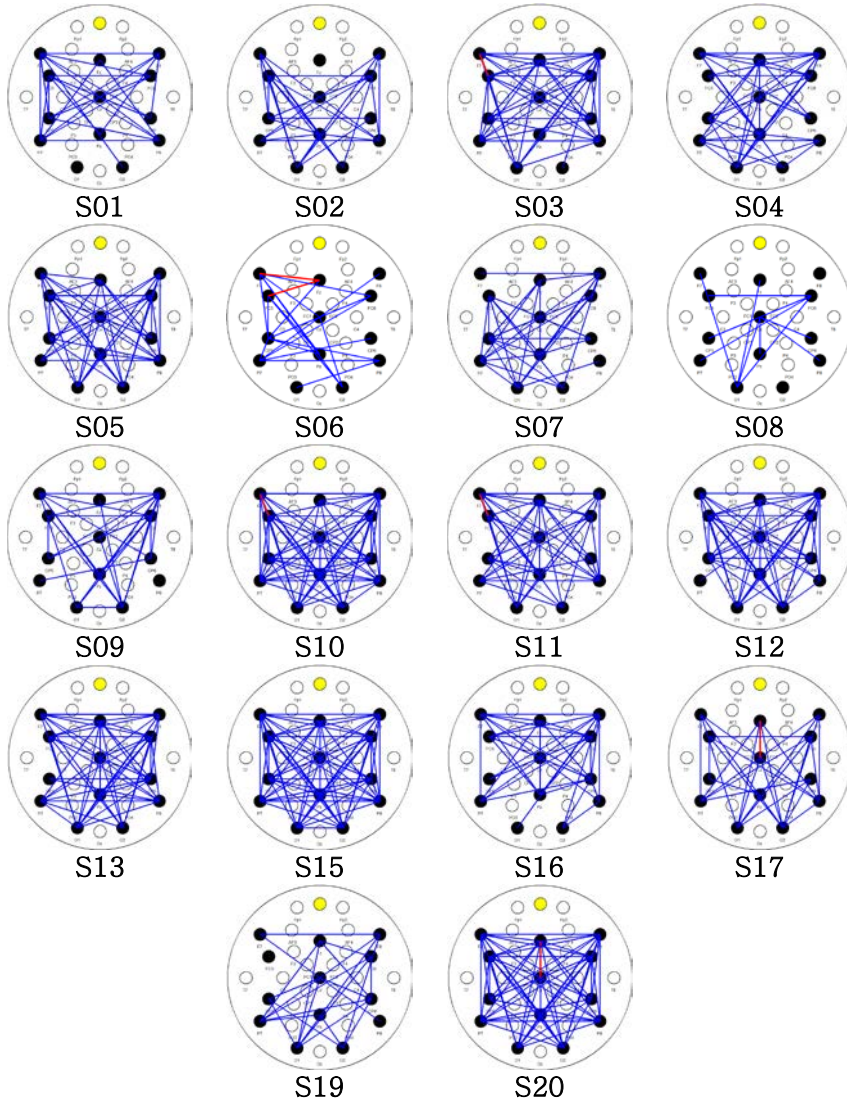


Figure 24. Theta coherence map of the subjects.

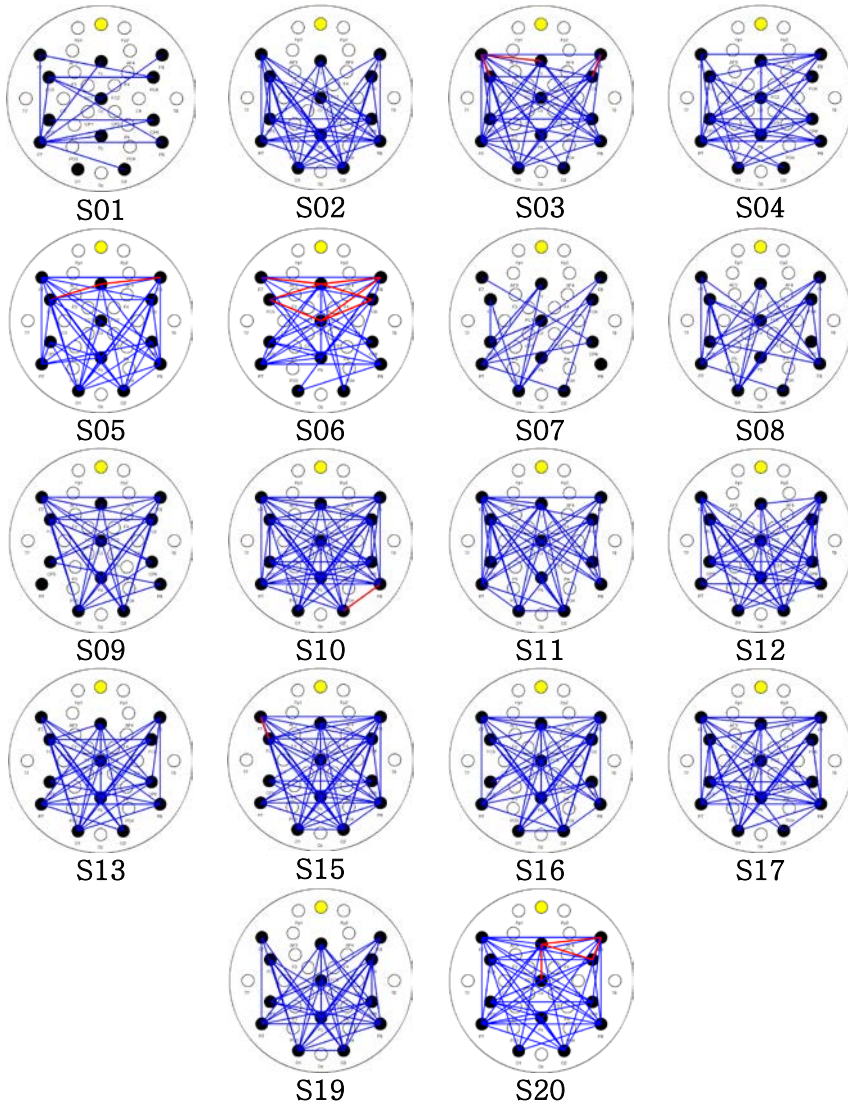


Figure 25. Alpha coherence map of the subjects.

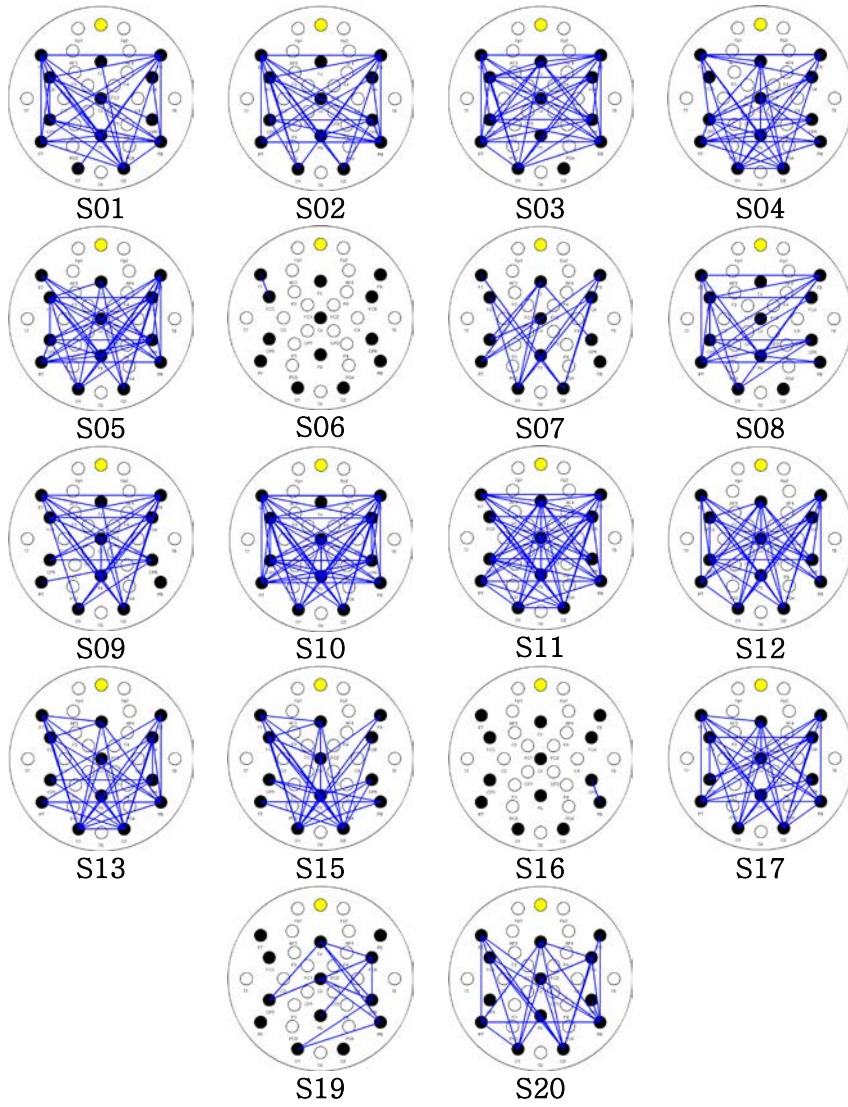


Figure 26. Beta coherence map of the subjects.

CHAPTER 4. DISCUSSION

In this thesis, the recognition system was designed using a systematic approach and the evaluation conducted was focused on the distinctiveness of the features used and their stability over time. Consequently, we measured the resting state EEG of 20 subjects on three different days at random intervals.

First, we evaluated the uniqueness of PSD and ZCOH by applying leave-one-out cross validation to the 30 trials used for the training set and selected the frequency range of the best performance to apply in the testing process. K-nearest neighbor classification was used. Using PSD, a best correct recognition rate of 98.83% was achieved in the frequency range 1-40 Hz and $k = 1$. For ZCOH, a best correct recognition rate of 99.67% was achieved in the 1-40 Hz frequency range with $k = 1$. We therefore concluded that PSD and ZCOH contain uniqueness of individuals.

Next, actual testing was conducted and the performance results evaluated using EEG measured in the other 2 days. We utilized

two recognition system modes, “Registered only” mode and “Imposter” mode. The former mode evaluates whether the test data are well classified to their correct class; therefore, correct recognition rate was calculated for overall performance, while precision, recall, specificity, and F-score were calculated for each subject. Averages of 81.35% and 80.04% for precision, 78.20% and 74.88% for recall, 99.04% and 98.81% for specificity and 0.78 and 0.75 for F-score were achieved with 80.39% and 75.70% correct recognition rate using PSD and ZCOH, respectively. The latter, “Imposter” mode is designed to add threshold in order to consider the case of other people trying to authenticate. The threshold was selected empirically. In the evaluation of this system, false acceptance rate, false rejection rate and half of total error rate was calculated. The lowest HTERs of 13.55% and 17.07% using PSD and ZCOH, respectively, were achieved.

Finally, by inspecting the results of the recognition test, statistical analysis of ZCOH was conducted in order to filter coherence values that guarantee stability and significance. Then,

conducting ANOVA of coherence measured on the three separate days, we filtered combinations for each subjects for each frequency band.

4.1 Factors that influence EEG

As mentioned in previous research, EEG is affected by various factors such as intake of caffeine or alcohol, alertness, stress level, emotions, sleep deprivation, diet condition, and even circadian rhythm. However, we assumed that variation in these factors was relatively less significant than its unique rhythms. In addition, regarding the practicality of applying EEG in the recognition system, minimum control of subjects was applied. They were only asked whether they were in normal condition.

4.2 Coherence characteristics in resting state

In this study, the stability of the coherence characteristics was evaluated from the perspective of reproducibility. Coherence has recently been viewed as the measurement of cognitive state in

clinical research. Research conducted by Lu et al. discriminated normal, mild cognitive impairment, and vegetative state by analyzing a network property composed of coherence of regions [24]. Kana et al. applied a similar method to normal and autism subjects and found that the characteristics of the connections between regions of brain are different [25]. The results in this thesis indicate that coherence has the possibility of uniqueness as a phenotype of individuals. However, interpretation of this coherence characteristic needs further evaluation.

4.3 Major drawback of using EEG as a biometric

Although EEG is viewed as a strong candidate for biometric authentication in respect of circumvention, the major drawback in collectability needs to be overcome. This drawback can be rectified both by hardware and software. As regards improvement of hardware, measuring of EEG without conductive gel and with high signal-to-noise ratio can be carried out. For software, recognition with less electrodes or extracting features that clearly distinguish individuals can be done.

In our experiment, a total of 30 channels were utilized, with conductive gel applied. This is not the best case from the aspect of practicality. However, reducing the number of channels also means reducing the number of features that can be extracted. However, in order to recognize more individuals, increase of features is inevitable. This tradeoff needs to be adjusted depending on how the recognition system is designed.

4.4 Limitations of the present study

In this study, the system was designed to recognize 20 subjects. Our main focus was extraction of features and classification with only data measured on the first day. Therefore, we did not filter the features that can lead to better performance in the recognition test. We evaluated only 20 subjects, but evaluations are needed with more subjects to recognize. Research conducted by La Rocca et al. recognized 108 individuals using the coherence information of 56 channels. However, this recognition was not evaluated on repeatedly measured EEG.

Another limitation is that the recognition system does not cover variations that occur as a result of mental impairment or abrupt cognitive state changes. We can assume that only healthy persons would use the recognition system; however, a systematic design that considers abrupt changes needs to be evaluated.

CHAPTER 5. CONCLUSION

In this thesis, the systematic design of a recognition system using short-time measured resting EEG measured on different days was presented and evaluated.

On the basis of the results of previous studies and validation of our data, we confirmed that power spectrum density and coherence contain unique characteristics that represent individuals.

To evaluate the recognition system, we utilized EEG measured on days different from those on which the data used in the training sets were obtained and compared the performance in two different modes. The design can be selected depending on the situation of the recognition system to be applied. As a consequence, different performance evaluations were conducted.

Although much remains to be done, as discussed in the previous section, we believe that this reliable short-time measured EEG identification/authentication system can be practically adopted for use in various applications.

REFERENCES

1. Ramya, T., et al. (2014). Personalized authentication procedure for restricted web service access in mobile phones. Applications of Digital Information and Web Technologies (ICADIWT), 2014 Fifth International Conference on the, IEEE.
2. Schneier, B. (2013). iPhone Fingerprint Authentication.
3. Nuwer, R. (2013). "Wristband unlocks your devices with your heartbeat." *New Scientist* 219(2933): 19
4. Sweatte, C. (2013). Method and System for Airport Security, Google Patents.
5. Corwin, D. J., et al. (2011). System and method for biometric signature authorization, Google Patents.

-
6. McEvoy, L., et al. (2000). "Test-retest reliability of cognitive EEG." *Clinical Neurophysiology* 111(3): 457–463.
 7. Barry, R. J., et al. (2007). "EEG differences between eyes-closed and eyes-open resting conditions." *Clinical Neurophysiology* 118(12): 2765–2773.
 8. Revett, K. (2012). "Cognitive biometrics: a novel approach to person authentication." *International Journal of Cognitive Biometrics* 1(1): 1–9.
 9. Haas, L. (2003). "Hans Berger (1873–1941), Richard Caton (1842–1926), and electroencephalography." *Journal of Neurology, Neurosurgery & Psychiatry* 74(1): 9–9.
 10. Broyd, S. J., et al. (2009). "Default-mode brain dysfunction in mental disorders: a systematic review." *Neuroscience & biobehavioral reviews* 33(3): 279–296.

11. Penttilä, M., et al. (1985). "Quantitative analysis of occipital EEG in different stages of Alzheimer's disease." *Electroencephalography and clinical neurophysiology* 60(1): 1–6.

12. Sethi, N. K., et al. (2014). "An elusive brain death diagnosis: You can't get there from here." *Neurology: Clinical Practice* 4(4): 272–273.

13. Davis, H. and P. A. Davis (1936). "Action potentials of the brain: In normal persons and in normal states of cerebral activity." *Archives of Neurology & Psychiatry* 36(6): 1214–1224.

14. Van Beijsterveldt, C. and G. Van Baal (2002). "Twin and family studies of the human electroencephalogram: a review and a meta-analysis." *Biological psychology* 61(1): 111–138.

15. Doppelmayr, M., et al. (1998). "Individual differences in brain dynamics: important implications for the calculation of event-related band power." *Biological Cybernetics* **79**(1): 49–57.

16. Nakanishi, I., et al. (2012). Evaluation of the brain wave as biometrics in a simulated driving environment. *Biometrics Special Interest Group (BIOSIG), 2012 BIOSIG-Proceedings of the International Conference of the, IEEE.*

17. Hu, B., et al. (2011). A real-time electroencephalogram (eeg) based individual identification interface for mobile security in ubiquitous environment. *Services Computing Conference (APSCC), 2011 IEEE Asia-Pacific, IEEE.*

18. La Rocca, D., et al. (2014). "Human brain distinctiveness based on EEG spectral coherence connectivity."

19. Kondacs, A. and M. Szabó (1999). "Long-term intra-individual variability of the background EEG in normals." *Clinical Neurophysiology* 110(10): 1708–1716.

20. Näpflin, M., et al. (2007). "Test-retest reliability of resting EEG spectra validates a statistical signature of persons." *Clinical Neurophysiology* 118(11): 2519–2524.

21. Aeschbach, D., et al. (1999). "Two circadian rhythms in the human electroencephalogram during wakefulness." *American Journal of Physiology–Regulatory, Integrative and Comparative Physiology* 277(6): R1771–R1779.

22. Amjad, A., et al. (1997). "An extended difference of coherence test for comparing and combining several independent coherence estimates: theory and application to the study of motor units and physiological tremor." *Journal of neuroscience methods* 73(1): 69–79.

23. Lu, C.-F., et al. "Relations of Progression in Cognitive Decline with Initial EEG Resting-State Functional Network in Mild Cognitive Impairment."

24. Kana, R. K., et al. (2014). "Brain connectivity in autism." *Frontiers in Human Neuroscience* 8: 349.

국문 초록

단시간 뇌파를 이용한 개별 인식 및 개인 인증

본 학위 논문은 비교적 짧은 10 초 동안 측정된 정상 상태의 뇌파를 이용해 20 명의 개별 간 구별과 함께 안정적인 재현이 가능한 개인 인증 시스템을 구성하고 검증하고 뇌파에 나타나는 간접성에 대한 재현 가능성을 분석했다.

다른 연구들에 따르면 정상 상태의 뇌파는 유전의 표현형이며 개별 인식에 사용될 가능성이 있다. 그리고 뇌파는 복제하기 어렵다는 점에서 개별 인식 및 보안의 수단으로 주목을 받았다. 주로 이용되는 특성은 뇌파의 주파수 별 나타나는 파워의 크기, 위치, 형태 등이었으며 정신적으로 건강하다면 가장 62 개월까지 그 특성이 유지되는 것으로 밝혀졌다. 그리고 최근 뇌파의 영역 간 상관도를 나타내는 간접성 특성 또한 개별 인식에 사용될 수 있는 가능성이 검증되었으나 재현 가능성이 검증되지 않았다. 그리고 인증을 진행하기 위해 뇌파를 1 분 이상 측정하거나 외부로부터 시, 청각 자극을 반복해서 집중해야 하는 제한 점이 있었다. 따라서 본 논문은 실질적인 뇌파 개인 인증 사용을 위해 측정 시간을 단축시키고 기존에 많이 사용되던 파워 특성

과 간접성 특성을 이용해 개인 인증 시스템을 구성하고 평가하였다. 다른 날 반복 측정된 데이터를 사용해 트레이닝과 테스트를 분리해 성능을 분석하였다.

우선적으로 파워 특성과 간접성 특성이 20 명 개별 특성을 반영하는 지 첫 날 측정한 데이터를 이용해 LOOCV 방법으로 평가하였다. 그 결과 파워 특성은 98.83%, 간접성 특성은 99.67%로 개별을 구별하였으며 두 특성은 고유성을 반영한다고 판단하였다.

인증 시스템은 트레이닝 데이터와는 다른 날에 측정한 뇌파를 이용해 테스트를 진행하였으며 개인 인증 시스템은 그 적용 상황을 감안해 두 가지 유형으로 구성해 각각 다른 지표로 그 성능을 평가하였다. 우선 첫 번째 유형은 등록된 사용자만 인증하는 경우에 대한 것으로 얼마나 각 개인을 제대로 판단하는지에 대해서 성능 평가를 진행하였다. 각각의 특성을 사용한 결과 전체 인증 정확도가 80.39%, 75.70%일 때 평균 81.35%, 80.04%의 정밀도, 78.20%, 74.88%의 민감도, 99.04%, 98.81%의 특이도, 0.78, 0.75 F-score 의 평균 성능을 나타냈다. 두 번째 유형은 침입자가 인증을 시도하는 경우를 가정하며, 추가적으로 기준을 도입하여 인증 여부를 판단하게 된다. 평가는 허위 인증 오류 (FAR), 허위 기각 오류 (FRR), 전체 오류의 절반 값 (HTER)을 통해 수행하였다. 그 결과, 파워와 간접성 특성을 사용했을 때 각각 13.55%,

19.98%의 HTER 을 성능을 나타냈다. 기존 1 분을 측정 한 다른 연구에
서는 51 명에 대해서 수행한 결과 14.3%의 HTER 의 성능을 나타내었
다. 본 연구는 20 명의 정상인에 대해 시간을 1/6 로 단축시켜 측정 한
뇌파로 구성된 인증시스템이 비슷한 성능을 나타내었다.

추가적으로 뇌파의 간섭성 특성이 재현 가능성이 있는지에 대해 통
계적 분석을 수행한 결과 각 뇌파 주파수 별 개인별 연결 특성이 다르
게 나타났다. 따라서 파워와 간섭성 특성 모두 개인 인증에 있어 유용
한 특성으로 사용할 수 있으며 실질적인 개인 인증 시스템에 응용될
수 있음을 검증하였다.

주요어 : 뇌파, 생체 인식, 개별 인식, 개인 인증

학 번 : 2013-21042